AD-A085 302 ILLINOIS UNIV AT URBANA-CHAMPAIGN ELECTROMAGNETICS LAB F/G 9/5
DIELECTRIC ANTENNAS FOR MILLIMETER-WAVE APPLICATIONS.(U)
MAY 80 S KOBAYASHI, R LAMPE, R MITTRA, S RAY DAAG29-77-G-0111
UNCLASSIFIED UIEN-80-3 ARO -14686.8-EL NL

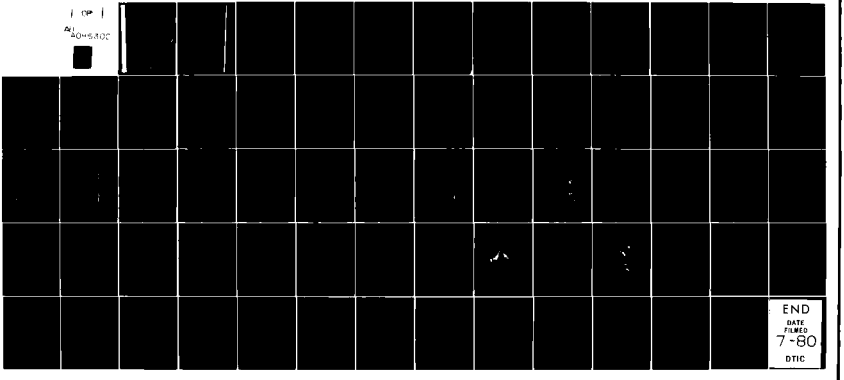

END
DATE FILMED
7-80
DTIC

(12)

DIELECTRIC ANTENNAS FOR MILLIMETER-WAVE APPLICATIONS

INTERIM TECHNICAL REPORT

S. KOBAYASHI
R. LAMPE
R. MITTRA
S. RAY

MAY 1980

U. S. ARMY RESEARCH OFFICE

GRANT NO. DAAG29-77-G0111

ELECTROMAGNETICS LABORATORY
DEPARTMENT OF ELECTRICAL ENGINEERING
ENGINEERING EXPERIMENT STATION
UNIVERSITY OF ILLINOIS AT URBANA-CHAMPAIGN
URBANA, ILLINOIS 61801

THE FINDINGS IN THIS REPORT ARE NOT TO BE CONSTRUED AS AN OFFICIAL DEPARTMENT OF THE ARMY POSITION, UNLESS SO DESIGNATED BY OTHER AUTHORIZED DOCUMENTS.

UNCLASSIFIED

SECURITY CLASSIFICATION OF THIS PAGE (When Data Entered)

REPORT DOCUMENTATION PAGE	READ INSTRUCTIONS BEFORE COMPLETING FORM
1. REPORT NUMBER 2. GOVT ACCESSION NO. AD-A085 302	3. RECIPIENT'S CATALOG NUMBER
4. TITLE (and Subtitle) DIELECTRIC ANTENNAS FOR MILLIMETER-WAVE APPLICATIONS.	5. TYPE OF REPORT & PERIOD COVERED Interim Technical Report
	6. PERFORMING ORG. REPORT NUMBER EM 80-3; UILU-ENG-80-2543
7. AUTHOR(s) (10) S. Kobayashi R. Lampe R. Mittra S. Ray	8. CONTRACT OR GRANT NUMBER(s) (15) DAAG29-77-G-0111
9. PERFORMING ORGANIZATION NAME AND ADDRESS Electromagnetics Laboratory / Department of Electrical Engineering University of Illinois, Urbana, Illinois 61801	10. PROGRAM ELEMENT, PROJECT, TASK AREA & WORK UNIT NUMBERS P-14686-EL (12) 47
11. CONTROLLING OFFICE NAME AND ADDRESS (11) U. S. Army Research Office Post Office Box 12211 Research Triangle Park, NC 27709	12. REPORT DATE May 80
	13. NUMBER OF PAGES 66
14. MONITORING AGENCY NAME & ADDRESS(if different from Controlling Office) (9) Interim rept.,	15. SECURITY CLASS. (of this report)
	15a. DECLASSIFICATION/DOWNGRADING SCHEDULE NA

16. DISTRIBUTION STATEMENT (of this Report)

Approved for public release; distribution unlimited.

(17) AROL (19) 14686.8-EL

17. DISTRIBUTION STATEMENT (of the abstract entered in Block 20, if different from Report)

(14) UIEM-80-3, UILU-ENG-80-2543

18. SUPPLEMENTARY NOTES

The findings in this report are not to be construed as an official Department of the Army position, unless so designated by other authorized documents.

19. KEY WORDS (Continue on reverse side if necessary and identify by block number)

Millimeter Waves, Dielectric Rod Antennas, Surface Wave Radiation, Leaky Wave Radiation, Frequency Scanning.

20. ABSTRACT (Continue on reverse side if necessary and identify by block number)

This report describes the results of an investigation of dielectric-based antennas for millimeter wavelengths. Two types of antennas have been studied, viz., ~~(i)~~ Uniform and tapered dielectric rod antennas of rectangular cross-section which radiate in the endfire direction; ~~(ii)~~ dielectric rods with discontinuities which perform as frequency scannable leaky-wave antennas. Experimental and theoretic design information and measured data on radiation pattern of both types of antennas are provided in the paper.

DD FORM 1 JAN 73 1473 EDITION OF 1 NOV 65 IS OBSOLETE

UNCLASSIFIED

SECURITY CLASSIFICATION OF THIS PAGE (When Data Entered)

408102 ll

UILU-ENG-80-2543

Electromagnetics Laboratory Report No. 80-3

DIELECTRIC ANTENNAS FOR MILLIMETER-WAVE APPLICATIONS

Interim Technical Report

S. Kobayashi
R. Lampe
R. Mittra
S. Ray

May 1980

U. S. Army Research Office
Grant No. DAAG29-77-G-0111

Electromagnetics Laboratory
Department of Electrical Engineering
Engineering Experiment Station
University of Illinois at Urbana-Champaign
Urbana, Illinois 61801

TABLE OF CONTENTS

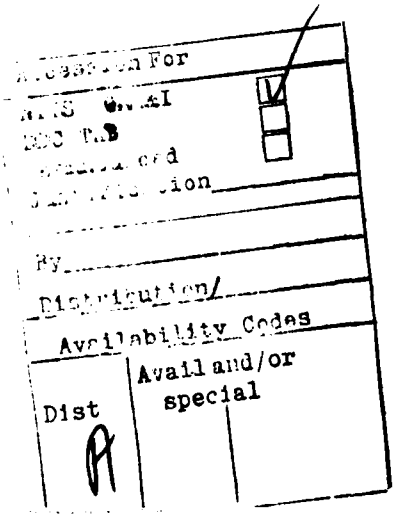

LIST OF FIGURES

I. INTRODUCTION

The surface-wave phenomenon along dielectric rods was known in the early twentieth century. In the late thirties, it was found that they are good directional radiators in the endfire direction. Most studies on dielectric rod antennas had been performed both experimentally and theoretically during the early fifties. Despite these investigations, the application has been rather limited due to their relatively low gain.

However, the recent progress of millimeter-wave dielectric integrated circuits and communication systems has generated an interest in developing front ends which are also fabricated from dielectric material so that they can be easily integrated with the remaining system. Although the design principles of dielectric rod antennas have already been completed for microwave frequencies, a simple scaling to the millimeter-wave frequencies does not seem to always be appropriate. Therefore, they are studied again experimentally here at the frequency of 80 GHz.

In addition to this type of rod antennas, the relatively short wavelength of millimeter-wave frequencies has made it practical to achieve another type of dielectric antenna, which has been referred to as periodically modulated surface-wave antennas. Periodical perturbations along a rod form an array. This type of antenna is characterized by its frequency-steerable beams. A primary study of this type of antenna is reported here.

In both cases, while most theoretical work has been done for the rods with circular cross sections, because of analysis, only the rods with rectangular cross sections are investigated and reported in this paper since our interest is mainly associated with millimeter-wave integrated circuits, for which a circular cross section is not preferable. However, antennas in this paper are fed from metal waveguides, and the ground-plane type of antennas is not discussed here.

II. DIELECTRIC ROD ANTENNAS

A. Aspects of Theoretical Analysis

Some examples of dielectric rod antennas are shown in Figure 1. The simplest one is just a rod inserted into a metal waveguide shown in Figure 1a. In earlier years, Mallach, Southworth, (referred to in Reference [1]), Kiely [2], and others made a model which assumed that radiation takes place from the surface s_r in Figure 2 and found the radiation pattern

$$F(\theta) = \frac{\sin \psi}{\psi} \tag{1}$$

where

$$\psi = 1/2\ k_o\ L\ (r - \cos\theta) \tag{2}$$

$$r = k_z/k_o \tag{3}$$

This theory predicts a null in the endfire direction for $\psi = 1/2\ k_o L\ (r-1) = \pi$. However, a null is rarely found in the endfire direction for lengths when $\psi = \pi$. In spite of some efforts to improve this theory [3],[4] the results were essentially the $\sin\psi/\psi$ type which fails at $\psi = \pi$.

Zucker [5] noticed that the radiation from the surface-wave structure takes place at discontinuities; i.e., mainly the feed point and the terminal point. He found that the radiation pattern, which is due to terminal radiation and is calculated by the integration over the terminal aperture s_t, is approximately expressed as $1/\psi$. This pattern does not have a side lobe. If the

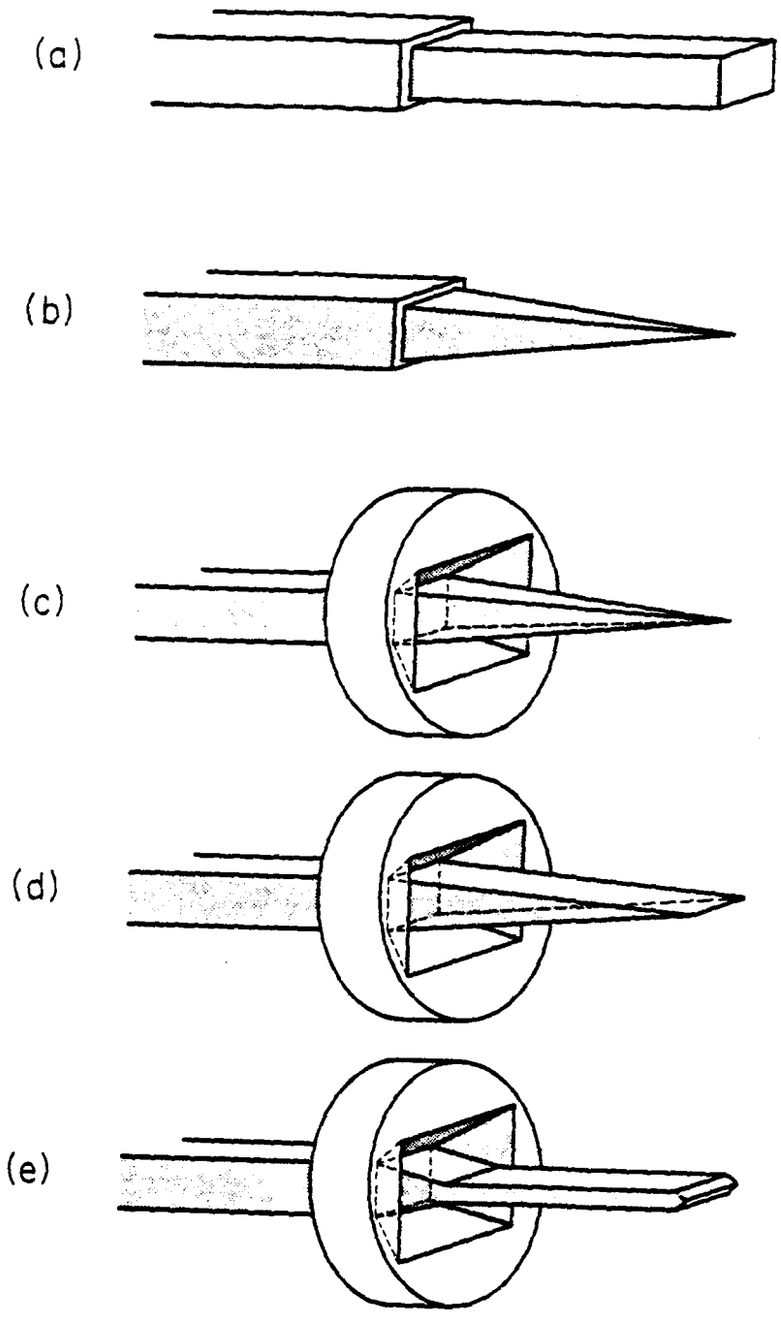

Figure 1. Examples of dielectric rod antennas with rectangular cross-sections.

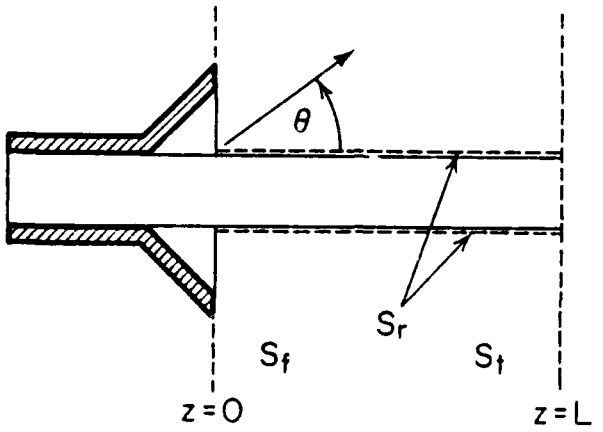

Figure 2. Schematic diagram of dielectric rod antennas.

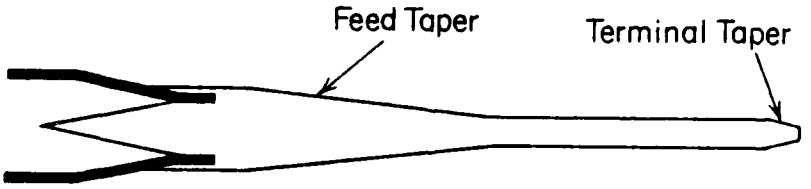

Figure 3. Basic configuration of maximum gain antennas.

radiation from the feed point is taken into account, side lobes result and they usually sharpen the main lobe [5]. Based on this fact, the design scheme for maximum-gain rod antennas was experimentally developed by Zucker. The basic configuration which is shown in Figure 3 is characterized by a feed taper, a straight section and a terminal taper. The feed taper is said to establish a surface wave along the straight section. The terminal taper reduces reflection and radiation which are caused by abrupt discontinuities.

Zucker's design principle seems to be useful, judging from the experimental results which were obtained in this work. However, it does not provide sufficiently accurate design information in the following aspects:

i. In order to determine the length of the rod, we have to know the propagation constant along the rod. But no appropriate method of calculation is available for rods with small rectangular cross sections. The Goell's method [6] seems to be the best, but it needs too much computation. The method of effective dielectric constant [7], the method of effective permeability,and their combination [8] have not yet been justified for rods with small cross sections. The Marcatili's method [9] and the method referred to in Itanami and Shindo's paper [10] are of little use in this region.

ii. Even if the propagation constant along a straight rod is calculated, difficulty remains in estimating the propagation constant along tapers.

iii. The leaky-wave radiation from the feed taper and the terminal taper must be taken into account. Radiation from tapers has been reported in the literature [11] and [12]. However, complexity discourages further study in applying it to dielectric rod antennas. Accordingly, fairly

gradual tapers are usually used on a cut-and-try basis.

iv. In addition to the leaky-wave radiation from tapers, the radiation from the abrupt discontinuity at the junction between metal waveguide and dielectric rod is another factor in determining the radiation pattern. Short feed horns are usually used to reduce this kind of radiation. However, the design principle of the feed horn is not clear.

Zucker's design principle is considered to be the best one so far in terms of its ability to achieve a high gain design. However, mechanical problems arise if they are applied in the millimeter-wave band. Zucker's type of tapering is not easy to make, especially in the case of a rectangular cross section, and the structure may lack mechanical strength. Moreover, the design of maximum gain may not be the biggest interest for many applications.

This paper does not attempt to give more precise design principles, but shows some experimental results. They might be helpful for actual designs of low side-lobe pattern antennas although they require tapering which makes analytical study almost impossible.

B. Design Factors

A metal waveguide fed dielectric antenna consists of three sections: a transition between the metal waveguide and the rod inside the metal waveguide, another transition section outside the metal waveguide, which we call a feed, and the rod extending into the air. For the first transition section, gradual tapering of a metal waveguide and/or dielectric rod is usually employed. A short horn or flare is frequently used to form a feed, and the main section of the antenna is just a rod either tapered or not. The terminal taper, which was mentioned in Zucker's design principle, is neglected here.

Considering the above general configuration, design factors are summarized in Table 1 and shown in Figure 4. There is a wide variety of dielectric material which can be considered of possible use for dielectric antennas. Physical strength, chemical stability, and ease of fabrication are the main factors in choosing the material in actual applications. However, this paper does not refer to those characteristics but only to the electromagnetic ones such as mismatch loss and propagation constants which determine the actual gain, beamwidth, side-lobe level, and so on. Since dielectric loss is not crucial, only the dielectric constant and shape of the rod are our concern.

Every design factor listed on Table 1, with the exception of the taper of the metal waveguide in the transition part, is taken into consideration in this paper. Since no taper was introduced to the metal waveguide, $A_m = A_r$ and $B_m = B_r$ throughout this paper.

C. Experimental Procedure

Since the design principles of this kind of antennas are not clear, most test antennas were made on a cut-and-try basis and the radiation pattern of each was recorded.

Test antennas were cut out of several different materials by using either knives, a milling machine or files. Soft material like teflon was not suitable for machining and was cut with very sharp knives. Polyethylene was machined with the accuracy of about 50 μm. A material called Stycast Hi K, which is brittle, required files and rand paper to fabricate it into small antennas.

Radiation patterns were measured by the equipment shown in Figure 5.

TABLE 1

DESIGN FACTORS FOR A DIELECTRIC ROD ANTENNA

Common Factors:

- Frequency range
- Metal Waveguide (cross-sectional dimensions)
- Material of the rod (dielectric constant, loss tangent, etc.)

Transition Factors:

- Length of transition
- Taper of the metal waveguide
- Taper of the rod

Feed Factors:

- Length of feed
- Flare angle of the horn
- Taper of the rod

Main Antenna Factors:

- Length of main antenna
- Taper of the rod (including the terminal taper)

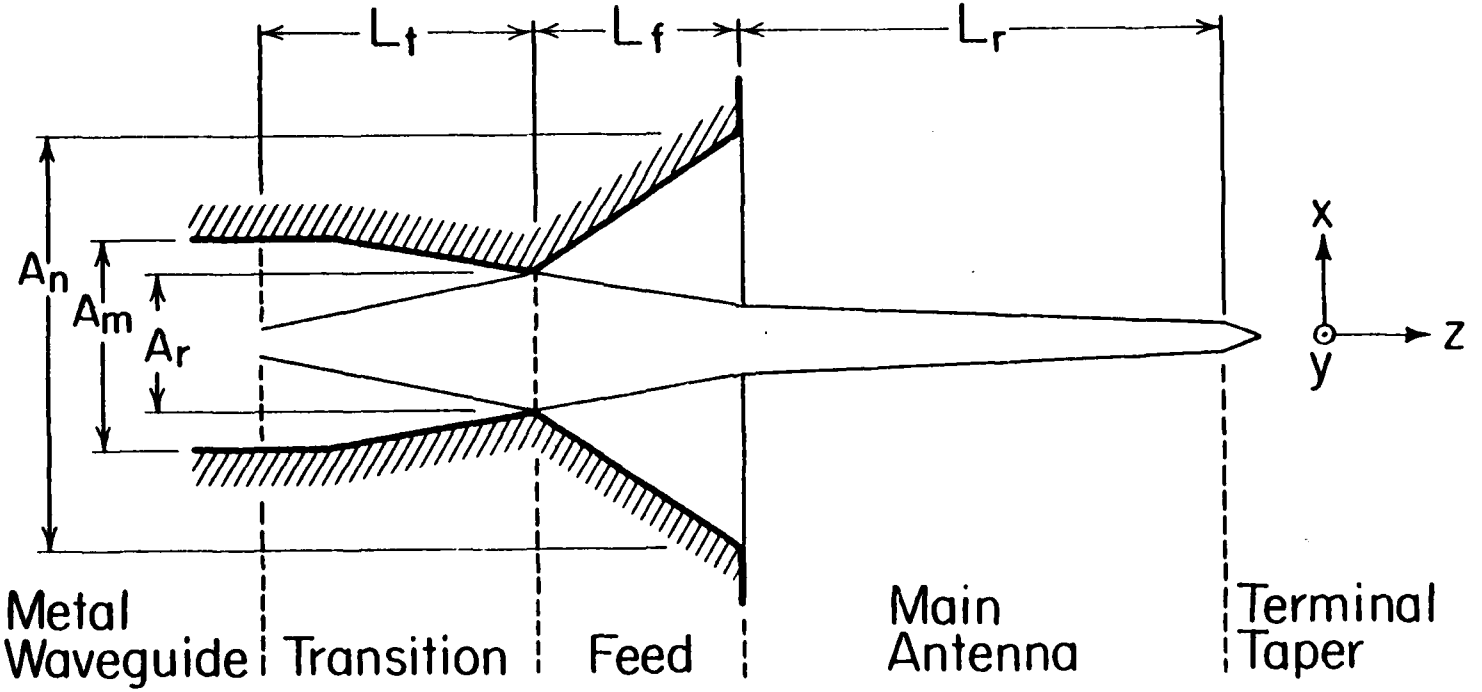

Figure 4. Dimensions of a dielectric rod antenna in xz-plane. In yz-plane, B_n, B_m and B_r are used instead of A_n, A_m and A_r.

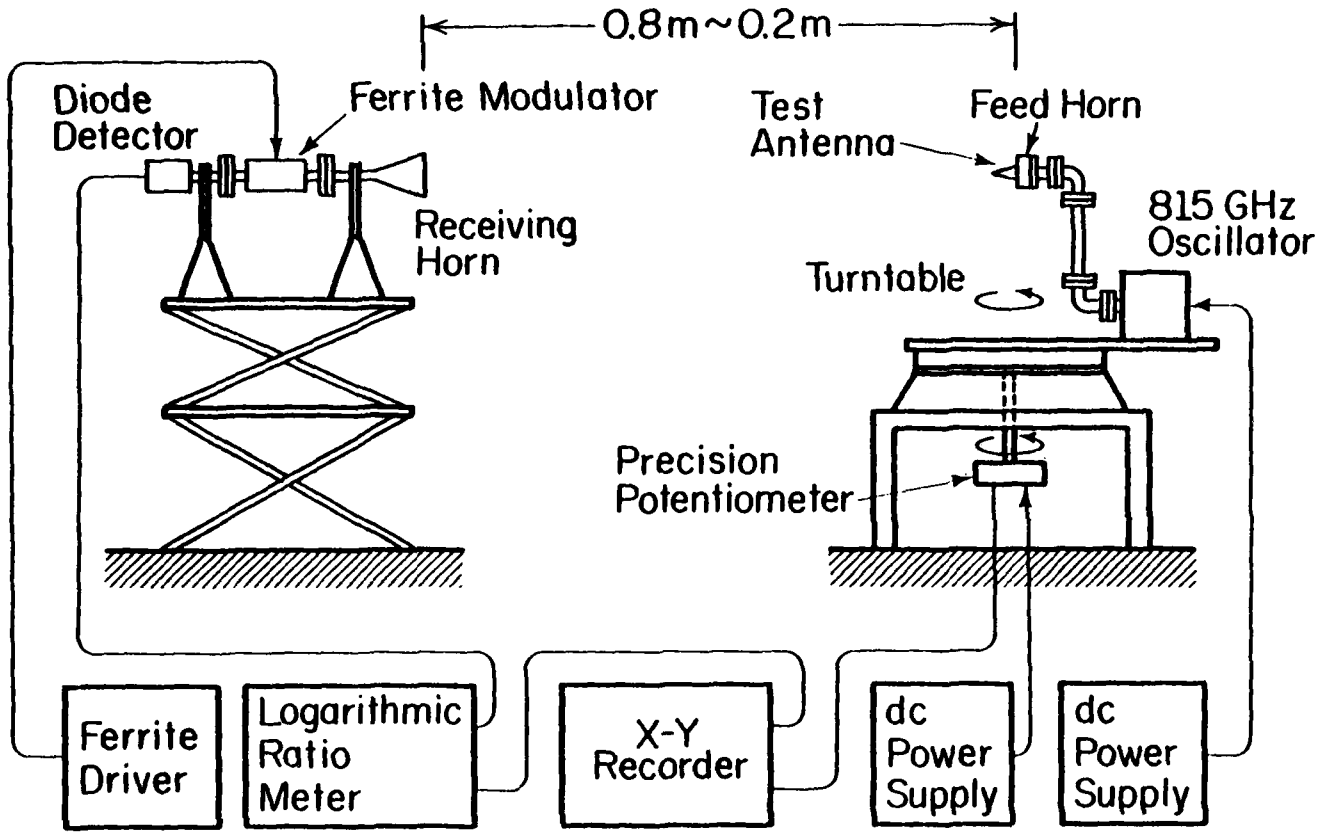

Figure 5. Radiation pattern measuring setup.

The equipment was set in a usual laboratory room in which the reflection from walls, tables, other equipment, human bodies, and etc. was found to be comparable to noise level.

A Fujitsu impatt oscillator was used as a source at a fixed frequency of 81.5 GHz — except for some earlier work for which a Hughes 41253H, micrometer-tuned impatt oscillator was used at the frequency of 80 GHz. For measurements at different frequencies, a Hughes 41051H impatt oscillator with less power, whose frequency is scannable in the range of 77 GHz to 87 GHz, was sometimes used. The oscillator with built-in isolator and a test antenna were put on a turn table with a degree scale and a precision potentiometer which provides the x-axis signal for a HP 7035B X-Y Recorder.

The transmitted signal was received by a rectangular horn antenna at the distance of about one meter (about 250λ). The received signal was modulated by a TRG E130 ferrite modulator with a 1 KHz square wave. The modulated signal was detected by a Hughes 47325H broadband diode detector, log amplified by a Micro-Tec 1006 logarithmic ratio meter, and used as a Y-axis input of the X-Y recorder.

A test antenna was installed on the transmitter side, and the radiation pattern in either the H-plane or E-plane was recorded on the X-Y recorder by rotating the table manually up to 360°. An ultramicrowave rectangular horn whose isotropic gain was calculated [13] to be 22 dB at 81.5 GHz was used as a gain standard to measure the actual gain. Since the loss in the transition between an RG 99/U metal waveguide and a dielectric waveguide, e.g., polyethylene rod, is estimated to be at most 0.2 ~ 0.3 dB if a 10 mm taper in the H-plane is used, the actual gain is very close to the directional gain.

For measurements of frequency characteristics, the return loss was measured using the equipment shown in Figure 6. A HP 202A low frequency function generator generates a saw-tooth wave and was used as a control signal and the X-axis input to the X-Y recorder. A Hughes 41051H impatt oscillator was driven by the Hughes 44017H sweep control unit output. Using a Fujitsu directional coupler and a Hughes 4732H broadband diode detector, the reflected power was detected, log-amplified, and recorded on the X-Y recorder.

D. Experimental Results

D.1 Transition in metal waveguide

A standard transition shown in Figure 7 was determined so as to be the best one at the frequency of 81.5 GHz for a polyethylene rod (ε_r=2.33) with a cross section of 3.1 mm x 1.55 mm. It was found experimentally that tapering in the x-z plane (H-plane) is better than that in the y-z plane (E-plane) and that good matching and good mechanical support are obtained by tapering only in the H-plane. For simplicity of fabrication, a linear taper in the H-plane is chosen as a standard transition and the length, L_t, was determined experimentally.

Figure 8 shows the return loss of characteristics of transitions with different length, assuming the feed and the main antenna are completely matched to the air. If the length is larger than 10 mm, the return loss does not increase because of the dielectric loss. A return loss of at least 14 dB (VSWR = 1.5) is achieved when the length is 10 mm. Therefore, mismatch loss is at most 0.18 dB over the frequency range from 79 GHz to 85 GHz.

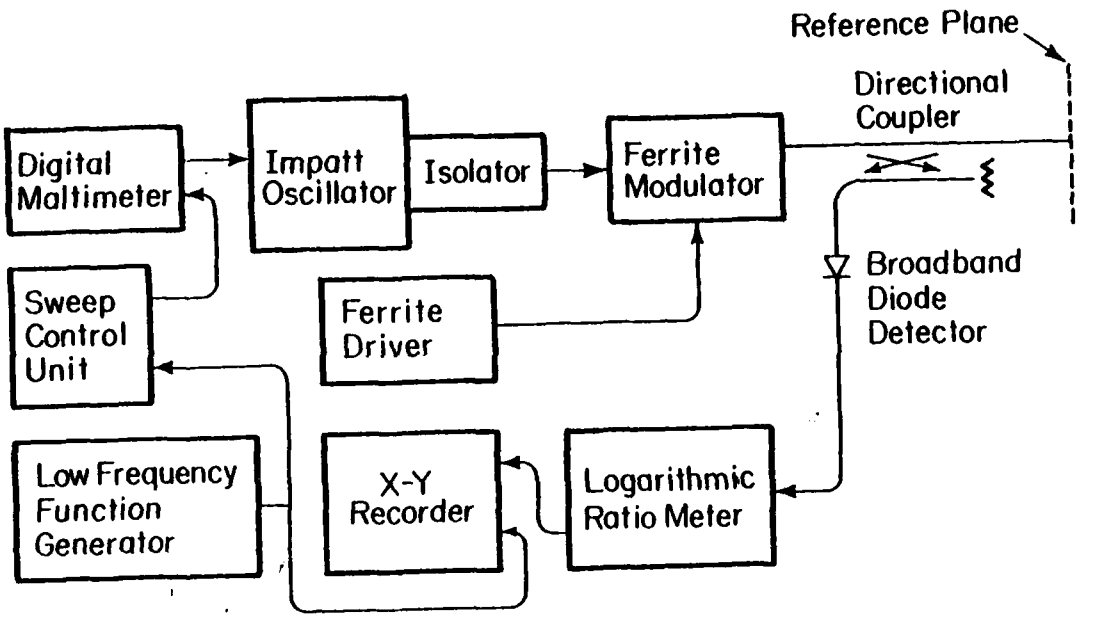

Figure 6. Return loss measuring setup.

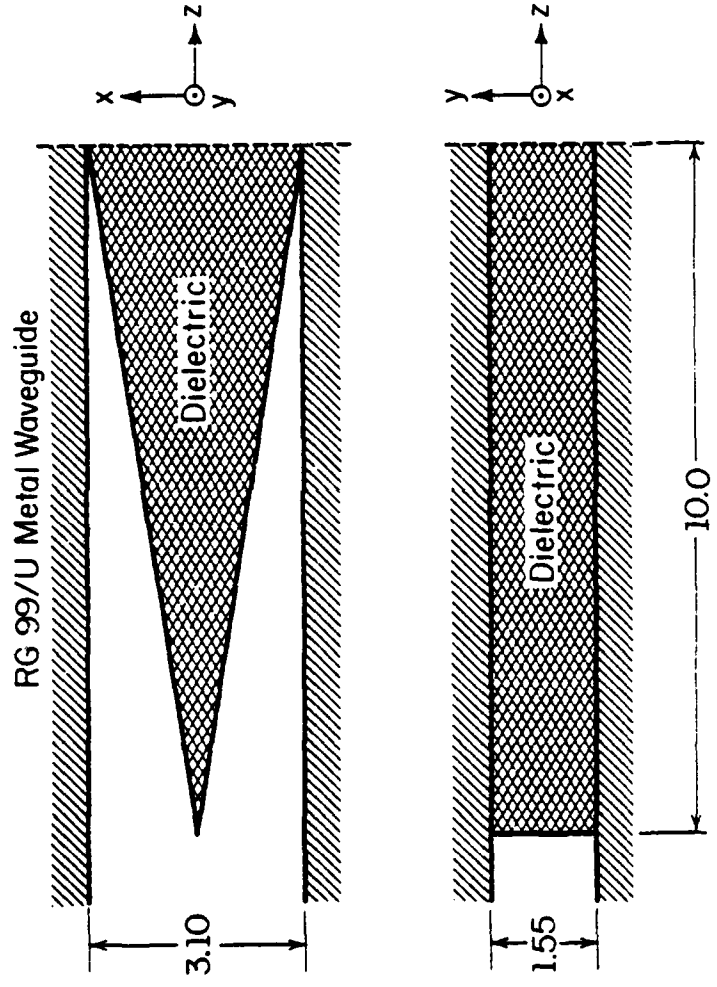

Figure 7. Standard transition.

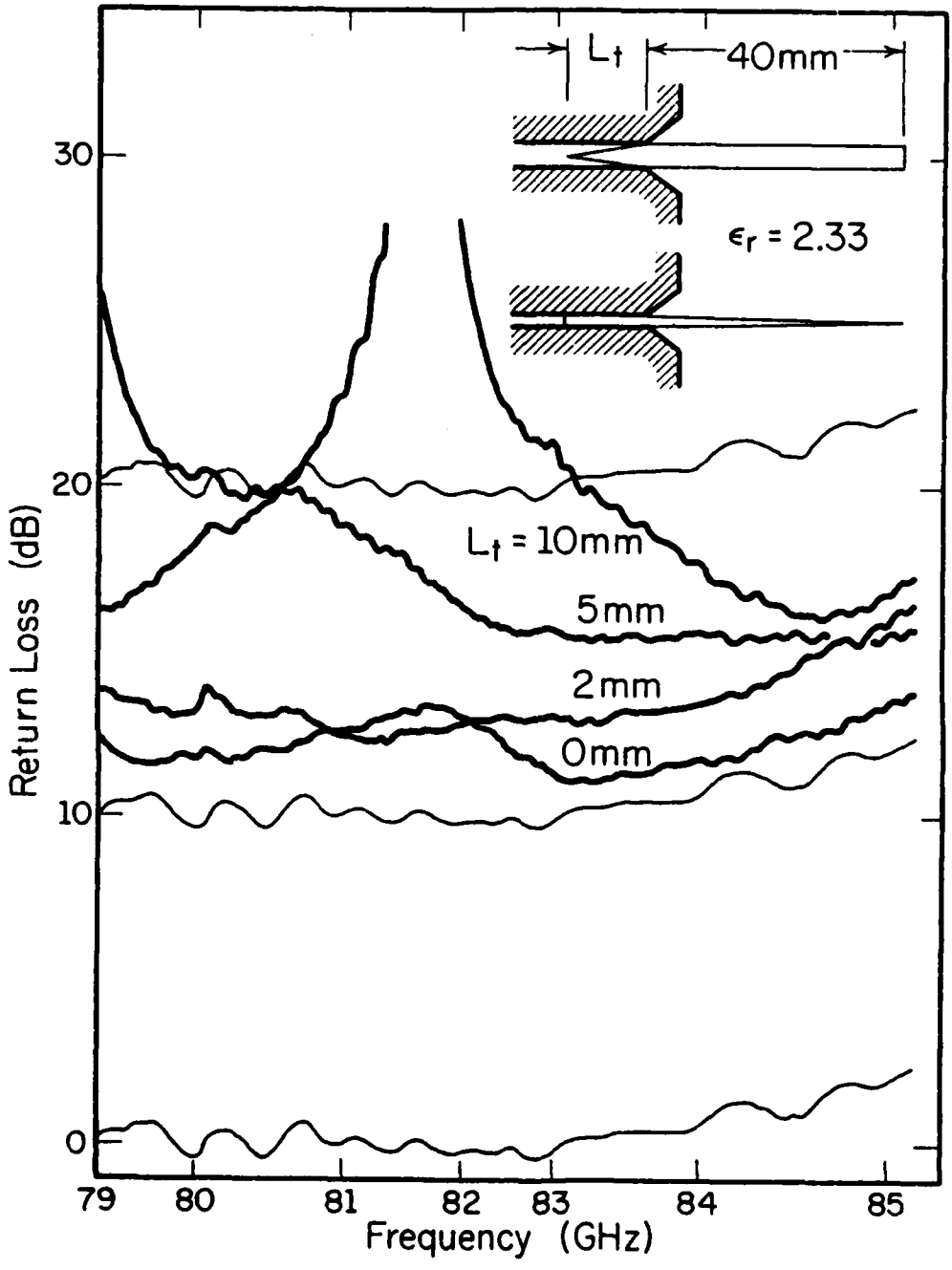

Figure 8. Return loss of transition.

This standard transition is used for all experiments unless otherwise mentioned.

D.2 Straight rod antenna without feed

The simplest dielectric rod antenna fed from a metal waveguide is a straight rod with a transition such as is shown in Figure 1(a). Since the radiation takes place only at the feed end and the terminal end, it is regarded as a two-element array whose element pattern is basically that of the rectangular aperture. If the length of the rod is much larger than the wavelength, we will see many lobes whose envelope is the radiation pattern of the waveguide aperture. Figure 9 shows an example of this sort of pattern. There will not be any application for this type of antenna.

D.3 Tapered rod antenna without feed

The radiation characteristics of a straight rod antenna can be improved by introducing a longitudinal taper to the main antenna part, which reduces the radiation and reflection from the abrupt discontinuity at the terminal end. However, leaky-wave radiation takes place from the taper in addition to the surface wave radiation and the radiation from the discontinuity at the feed end. For our experiments, the rods were tapered in both the E- and H-planes linearly to a point, which resulted in radiation patters as shown in Figure 10. The surface wave radiation is well emphasized in the main lobe. The interference between these three different types of radiation seems to distort the main lobe, but it is almost impossible to control the distortion or the beam shape because of complexity of the radiation mechanism. Moreover, side lobes due to feed end radiation are relatively high. Therefore, it is expected that the reduction of feed-end radiation might also improve the shape of the main lobe.

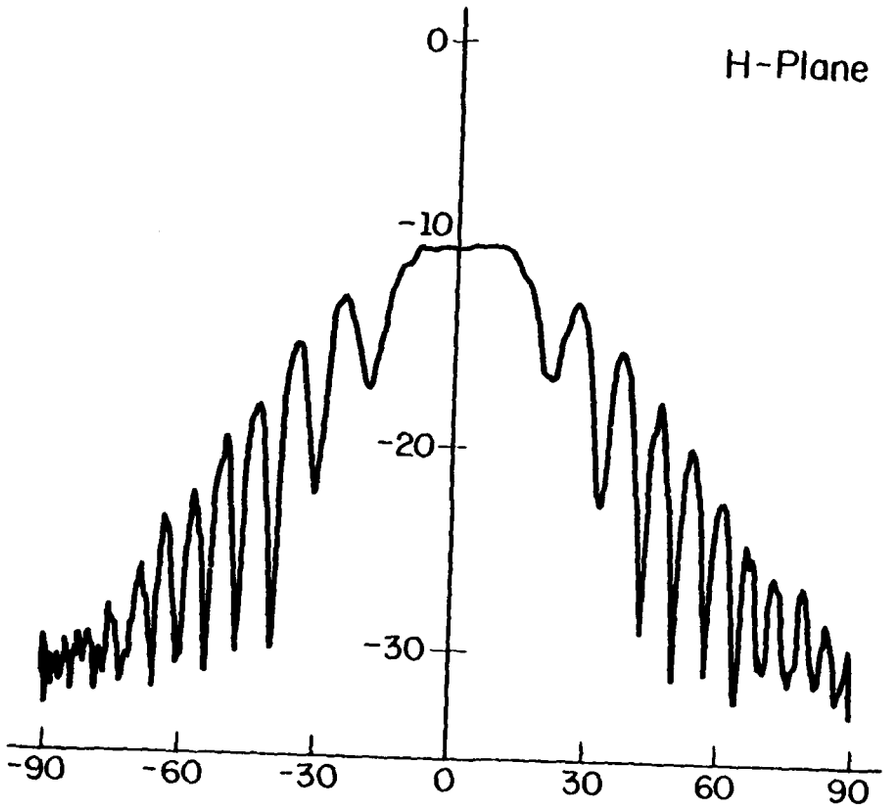

Figure 9. Radiation pattern of straight rod antenna without feed. (Gain = 11.9 dB)

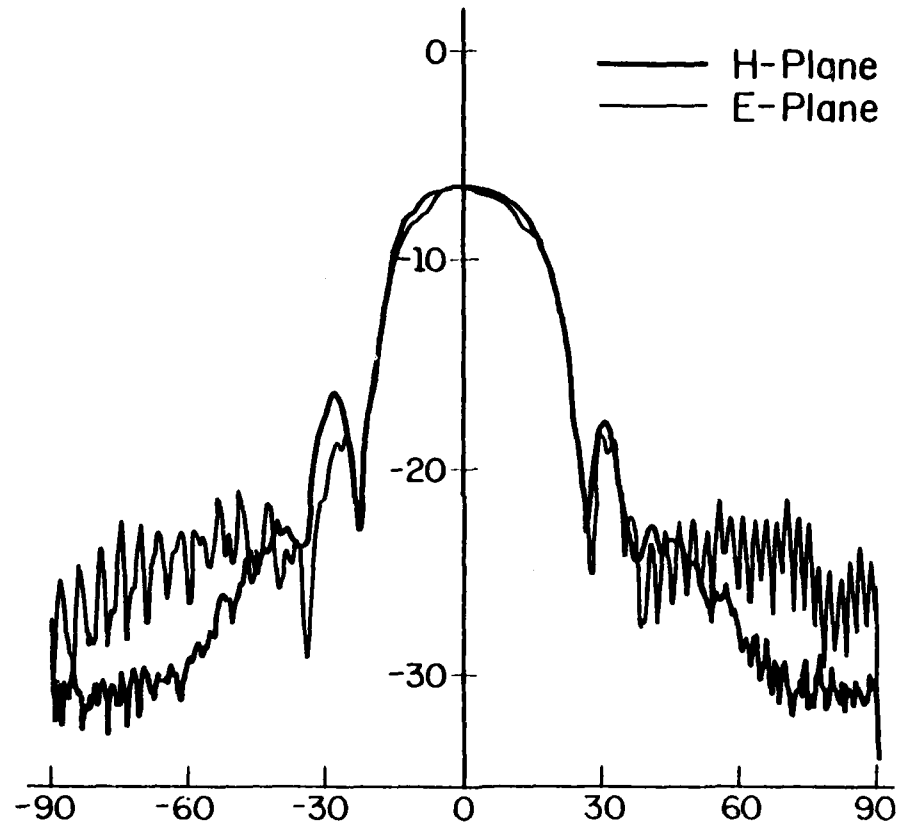

Figure 10. Radiation pattern of rod antenna tapered in both planes without feed horn. (Gain = 15.6 dB)

D.4 Tapered rod antenna with feed horn

In order to reduce the feed-end radiation and to increase the efficiency of launching the surface wave onto the rod, an E-band launching horn developed by Trinh, Malherbe and Mittra [14] was used as a feed horn. The dimensions of the horn are shown in Figure 11, and the measured gain of the horn itself is 17.3 dB at 8.15 GHz. For simplicity, the rods were tapered in both the E- and H-plane linearly to a point. Figure 12 shows the radiation pattern of a 20 mm teflon rod antenna ($\varepsilon_r = 2.1$). The feed-end radiation is significantly reduced and a remarkable side-lobe level of lower than -25.5 dB from the main beam is achieved. The gain (17.0 dB) is slightly lower than that for the feed horn (17.3 dB), and the half-power beam width (30.0°) is larger than that for the feed horn (26.9°). However, the 26 dB beam width of this antenna is only 72°, while that for the horn is about 115°. The remarkable side-lobe characteristics and the very steep off-main-beam attenuation are the features of a relatively short tapered rod antenna with a feed horn.

If the length becomes larger, the gain increases but the side lobe level also goes up. The dependency on the length of the rod is discussed in the following section.

D.5 E-plane tapered rod antenna with feed horn

The rods mentioned in section 3 and 4 are tapered in both the E- and H-planes for experimental convenience. But, from the mechanical point of view, this structure is neither strong nor easy to machine. It was found from experiments that tapering in only the E-plane improves the mechanical situation with no sacrifice in antenna characteristics, and even sometimes with a little improvement. But, H-plane taper was always worse than both-plane taper. This is explained by observing the local wave number along the rod. Figure 13 shows the normalized local wave number curves calculated

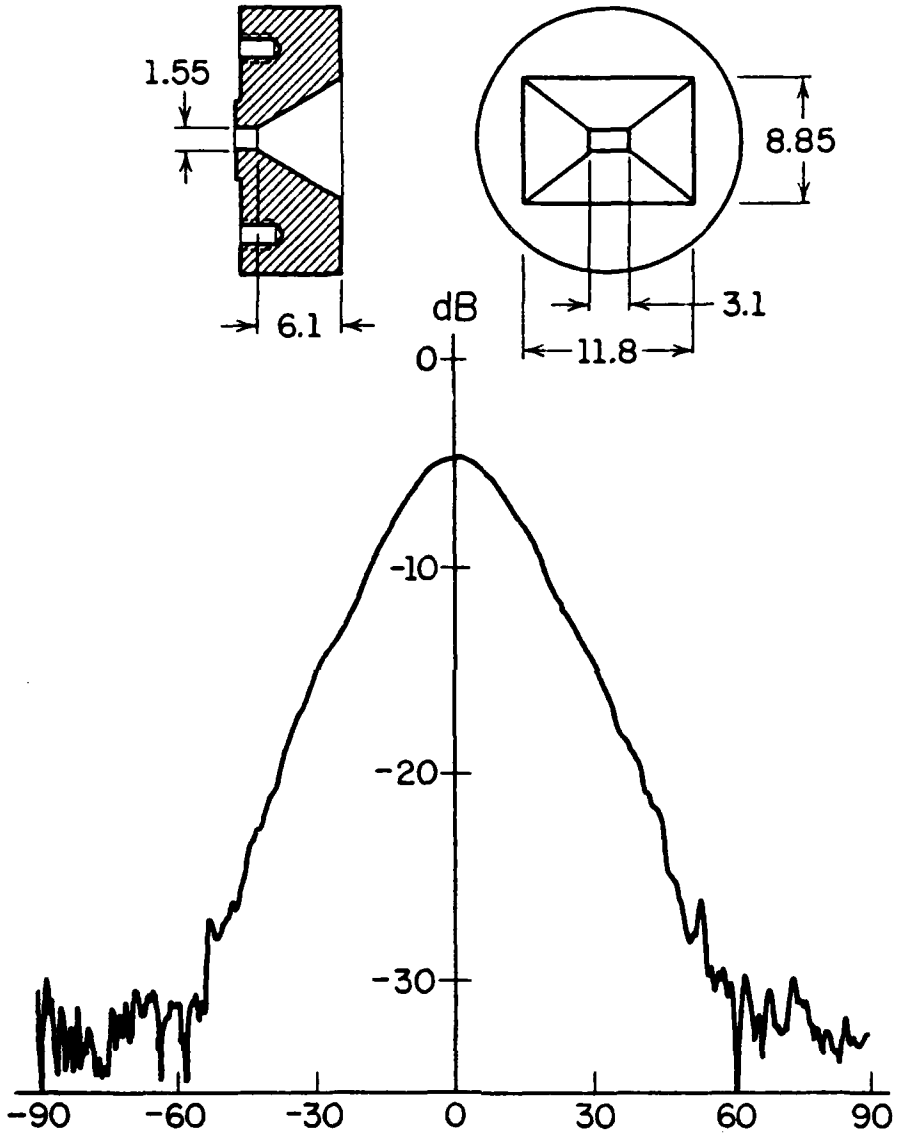

Figure 11. Inside dimensions of the feed horn and its radiation pattern in H-plane.

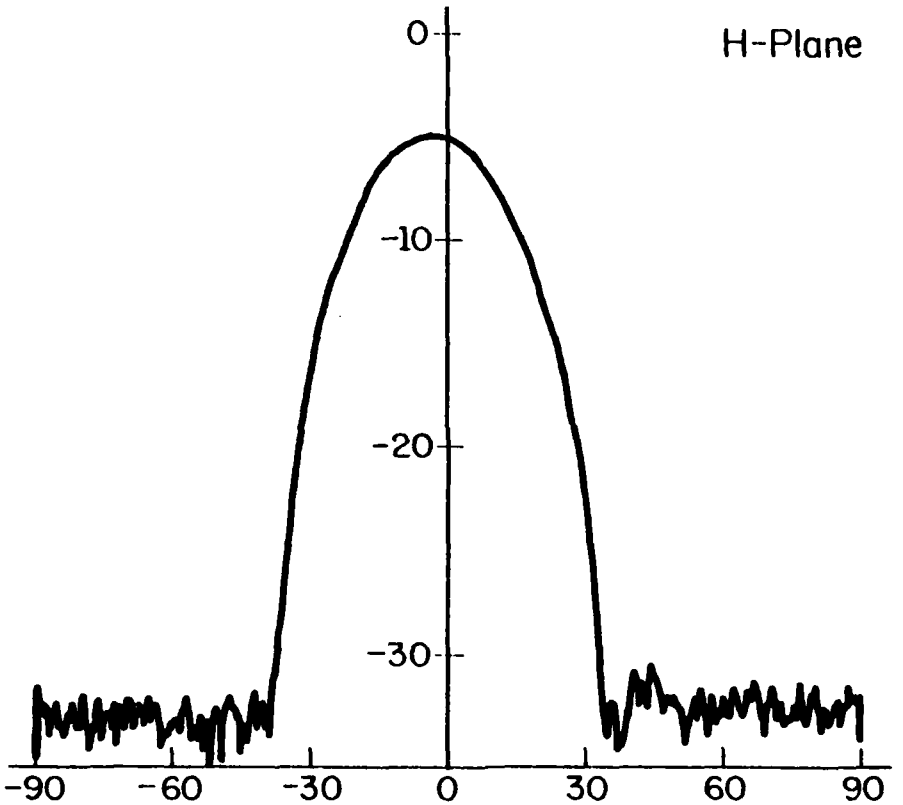

Figure 12. Radiation pattern of rod antenna tapered in both planes with feed horn. (Gain = 17.0 dB)

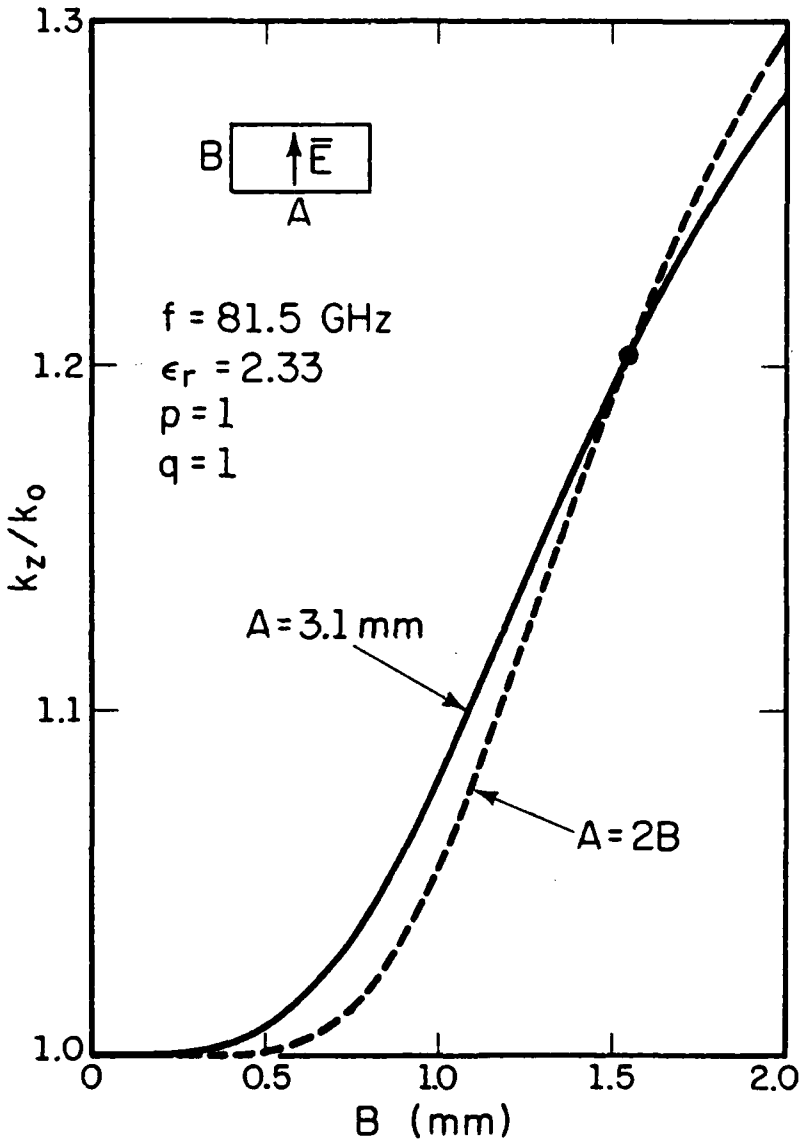

Figure 13. Normalized local wave number of a rod tapered in E-plane.

by the method of effective dielectric constant for an E-plane taper and a both-plane taper, while Figure 14 shows the curves for an H-plane taper and a both-plane taper. Two curves in Figure 13 are obviously more similar than those in Figure 14, which is usually true because of the aspect ratio of metal waveguides. Since it is the local wave number curve along a rod that seems to determine the radiation characteristics, it is expected that an E-plane taper behaves very similarly to a both-plane taper.

In addition, Figure 13 and Figure 14 tell us more. Since a rod is not seen if the wave number along the rod is very close to that in free space, an E-plane taper can be truncated, but an H-plane taper cannot. This is another advantage of the E-plane taper. Since tapering in only one plane and using polyethylene as a material allowed us more accurate fabrication, the length-dependency of E-plane tapered antennas was measured. Figure 15 shows the results.

If the rod is as short as the length of the feed horn, the horn is dominant to determine the radiation pattern. The gain is lower than that of the horn itself and the beam is wider. As the length increases, the gain increases monotonically and the main beam becomes sharper. In Figure 15, L = 25 mm is the length for which the side lobe level is extremely low and the off-beam attenuation is large. If the rod becomes longer, a distortion of the main beam pattern appears, which finally results in high side lobes.

If we need very good side-lobe characteristics, and don't need very high gain, a short antenna, such as L = 25 mm, of this type is a good choice. If we need a relatively higher gain, we may choose an antenna which is described in the following section or, if possible, we may choose other antennas than dielectric rod antennas.

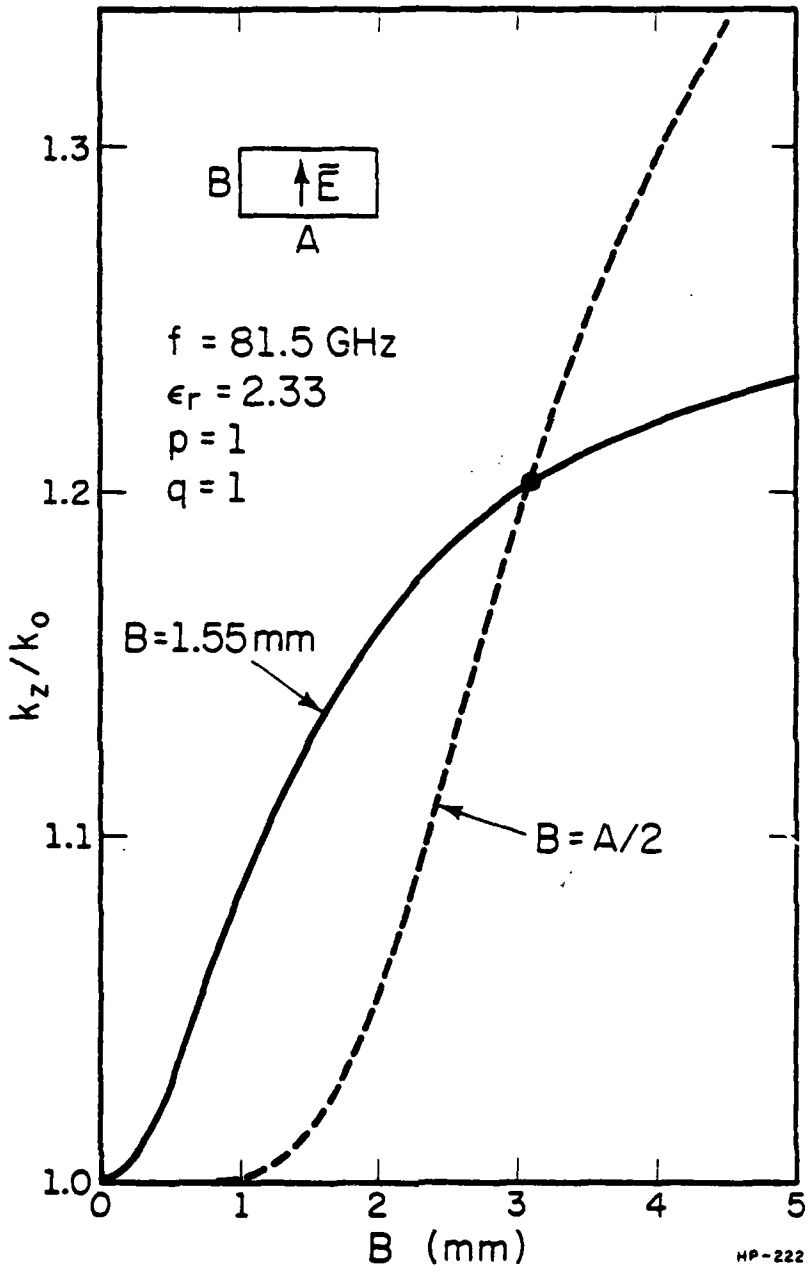

Figure 14. Normalized local wave number of a rod tapered in H-plane.

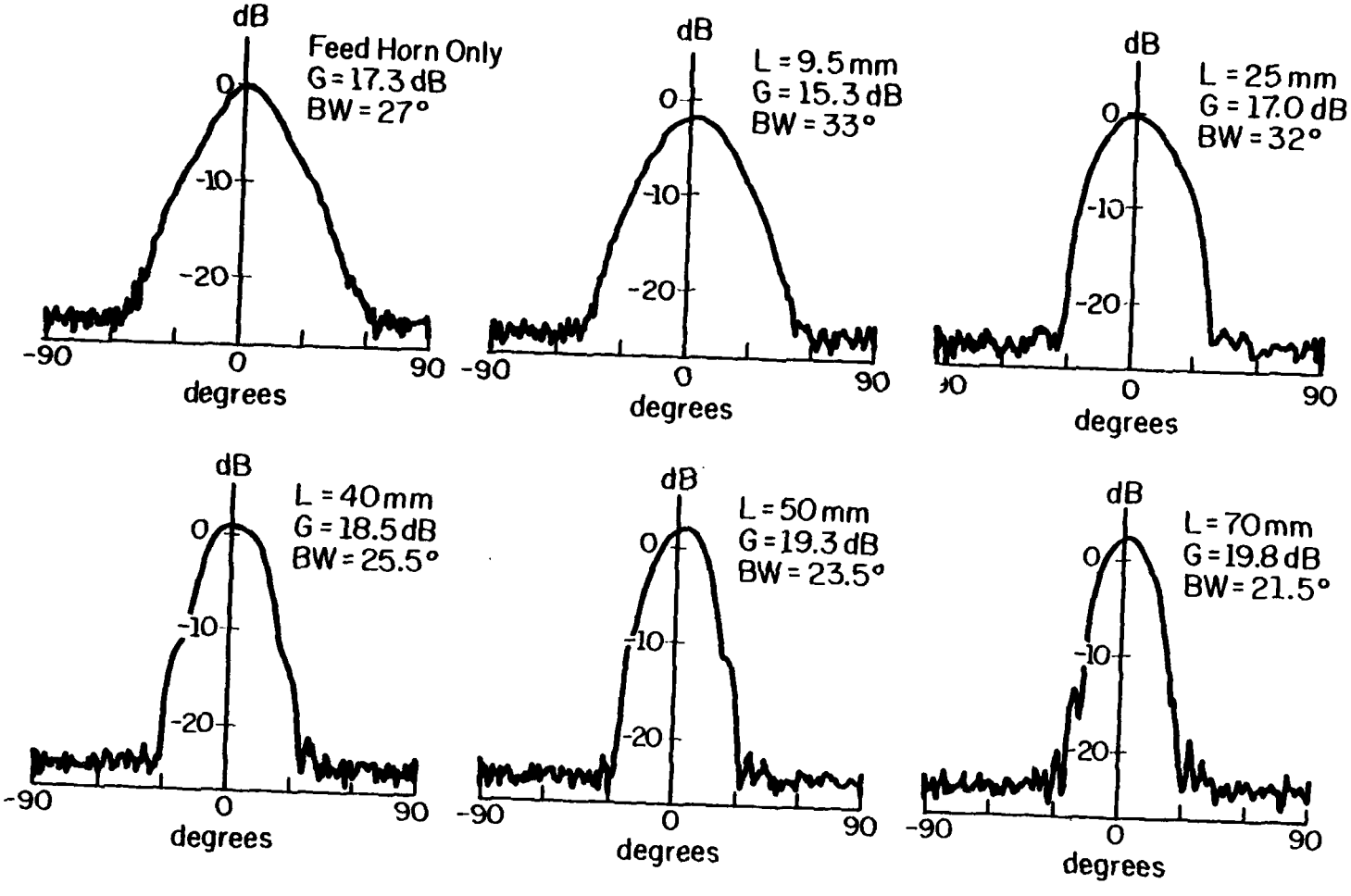

Figure 15. Radiation patterns of E-plane-tapered rod antennas with feed horn.

D.6 Zucker's maximum gain rod antenna

A method of design, which is summarized in Appendix A, was developed based on the Zucker's design principles [5] for maximum gain antennas. Using this method, several test antennas were fabricated and the patterns were recorded.

Figure 16 shows H-plane and E-plane patterns of a 40 mm long antenna. Although the gain (19.1 dB) is not as high as the expected gain (20.2 dB), it is still 0.6 dB higher than that for a linearly tapered rod of the same length. The half-power beamwidth is 15.9° in the H-plane and 16.1° in the E-plane. This is very close to the expected value (15.9°). Since the beam width of the antenna discussed in Section D.5 is 25.5°, it is apparently much improved. However, this is at the expense of the side lobe characteristics. The side-lobe level is as high as -6.2 dB and the envelope of the side lobes is much wider than the radiation pattern of the antenna described in Section D.5. Since the improvement in gain is not very large in this case, and the side-lobe pattern is sacrificed, the design principles used here will not be appropriate for all applications.

Zucker's principle is typically useful for designing a very long rod antenna and in the application of this principle, it often leads to a very thin cross-section for the antenna because of the limit in the phase difference of Equations (A.1) and (A.2).

In order to test the feasibility of realizing the Zucker antenna, a 140 mm long rod was fabricated. To keep the rod straight, a different cross section (A = 12.7 mm) was used and the whole antenna was sandwiched by two blocks of low-loss styrofoam because the calculated thickness B' of the main antennas section was only 0.35 mm. The radiation pattern of this antenna is shown in

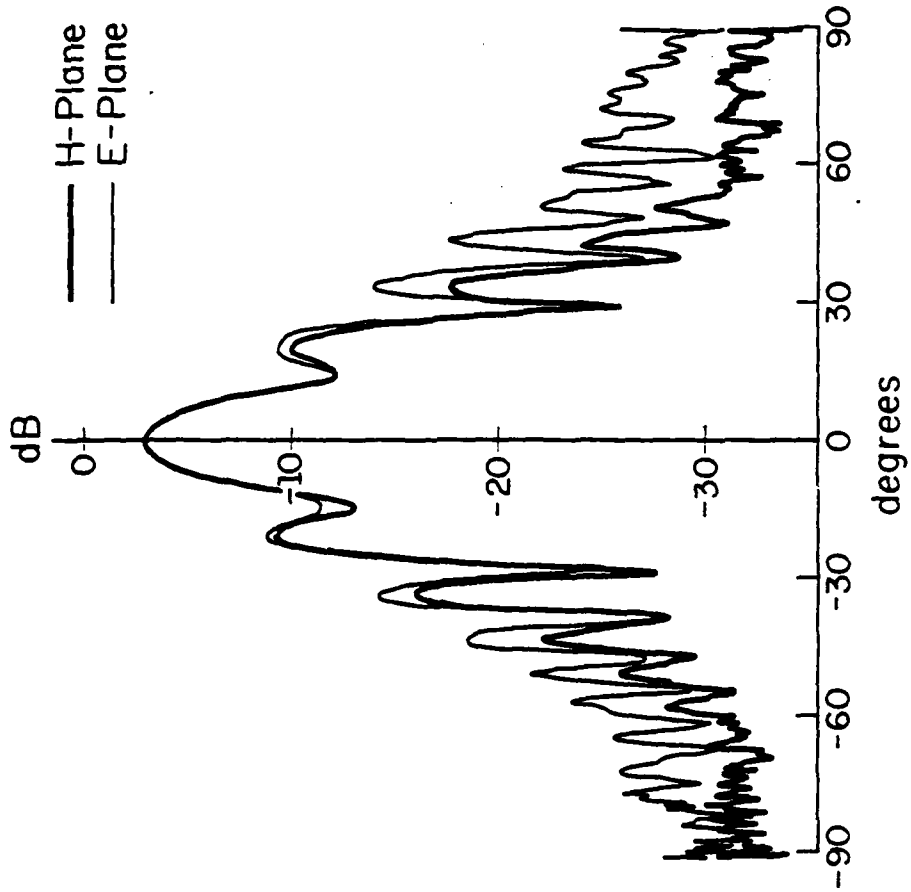

Figure 16. Radiation pattern of Zucker's maximum gain rod antenna (L = 20.0 mm, Gain = 19.1 dB)

Figure 17. The gain is 24.9 dB, which is very close to the expected maximum gain of 25.2 dB and the beamwidth is 8.1° in the H-plane and 6.2° in the E-plane. Since the expected value of the beam width is 8.2°, a better explanation of this narrower beam is needed.

The level of the first side lobe is -6.7 dB in both the E and E-planes. The other side lobes are fairly small in the H-plane, but higher in the E-plane. This is probably caused by the irregular cross-section of the main antenna section which is 12.7 mm in the H-plane and 0.35 mm in the E-plane. It is also found that the main beam is sharper in the E-plane in spite of the smaller size of the main antenna section in the same plane.

D.7 Rod antenna with higher dielectric constant

Although teflon and polyethylene were used in most of the experiments, (each of which is widely available, has sufficiently low dielectric constant, and possesses enough physical strength), the characteristics of the antennas which are made of higher dielectric constant material were also measured, because in general, they are physically stronger.

Using a material called Stycast Hi K with relative dielectric constant 6, several linearly tapered rods whose length, L, varies from 11 mm to 30 mm, were fabricated and their characteristics were measured. In a word, none of these antennas were satisfactory. The rods tapered in the H-plane showed the worst patterns. The gain of these antennas is very low, the side lobes are almost comparable to the main lobe, and the main lobe is distorted and in most cases it is split into two. The E-plane tapered rods have higher gain, but it is not as high as that for a polyethelene rod of the same length. Furthermore, the side-lobe characteristics are better than those for H-plane tapered ones, but the main beam is still distorted and sometimes split in the E-plane.

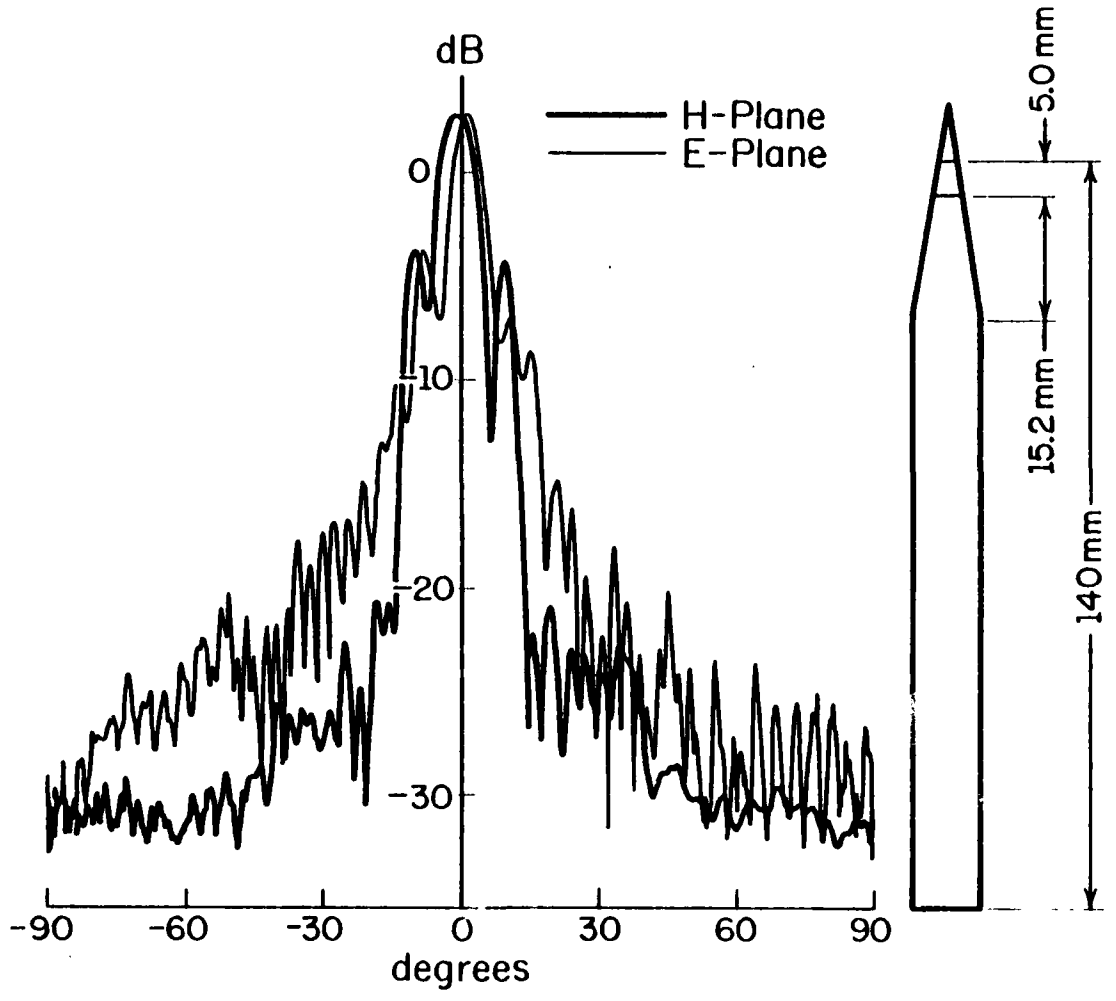

Figure 17. Radiation pattern of Zucker's maximum gain rod antenna. (L = 140 mm, Gain = 24.9 dB)

There are a few possible reasons for these undesirable characteristics: First, the local wave number in the direction of the rod at the feed end is too large. Even if we taper the rod, the phase difference condition described in Appendix A will be satisfied in a very short length of the rod. The rest of the length makes the rod violate the phase difference condition, which leads to a lower gain and a distorted main beam. Second, multimoding may cause the radiation pattern to suffer. These two problems can be solved by introducing a metal waveguide taper, which makes the rod cross section smaller. The third reason for this worse antenna performance is the degradation of the transition section. The reason for the bad characteristics of the H-plane tapered rod antenna may be the intensive leaky-wave radiation near the termination where the local wave number decreases very rapidly.

It may be possible to improve the characteristics of a rod antenna with higher dielectric constant. However, Zucker's principle discourages the use of higher dielectric constant material. The principle says that the higher the gain, the thinner the rod, which somewhat cancels the physical strength of the higher dielectric constant material. Moreover, the maximum gain depends only on the length of the rod, which implies that we need to find a material which is physically strong enough and whose dielectric constant is as low as possible. Or, if the material is too soft to keep its shape, it may be helpful to embed the whole antenna in a much lower dielectric constant material like the styrofoam which is mentioned in Section D.6.

D.8 Summary of dielectric rod antennas

Several types of rod antennas were experimentally investigated in the millimeter-wave frequency band. The gain and beamwidth of the rod antennas presented in this paper are shown in Figure 18 and Figure 19, respectively.

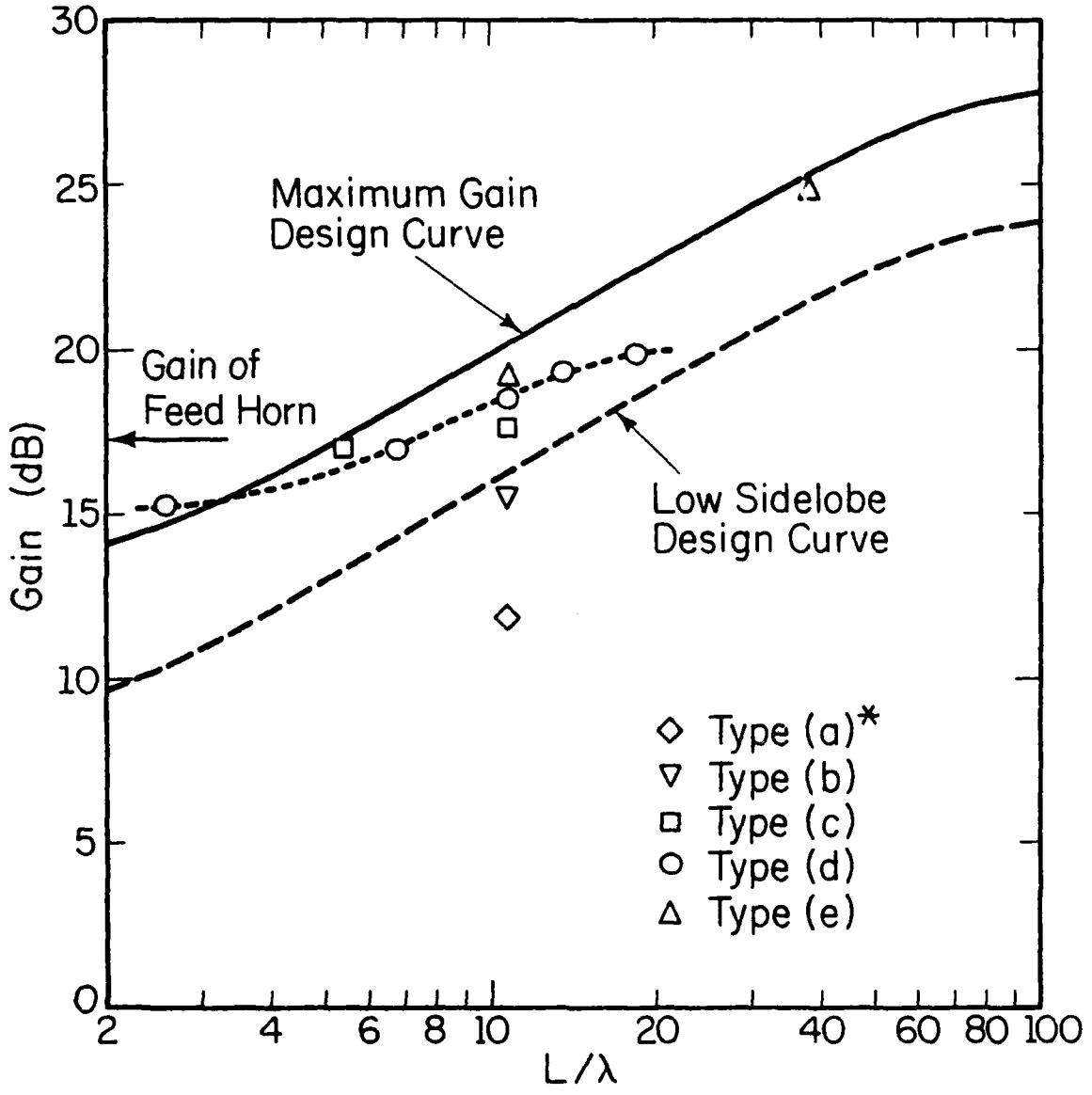

Figure 18. Gain of different types of antennas.

* See Figure 1

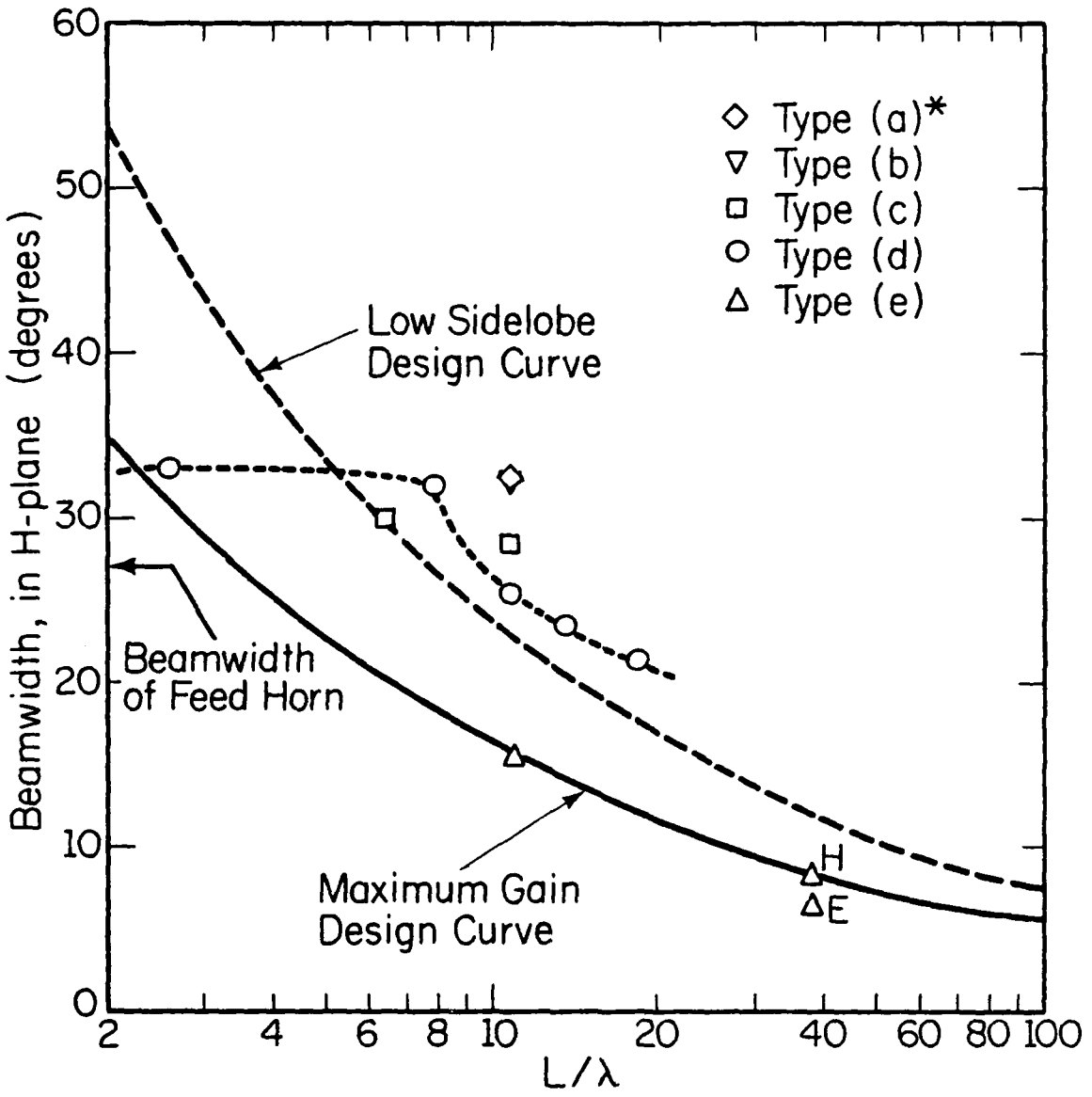

Figure 19. Beamwidth of different types of antennas.

* See Figure 1

The solid line shows the gain or the beamwidth of Zucker's maximum gain antenna. The broken line is for the low side-lobe design. The dotted line shows the curve for the antenna which is tapered linearly in the E-plane. The improvement of the characteristics of a 40 mm long antenna by changing the shape is summarized in Table 2.

TABLE 2

COMPARISON OF DIFFERENT TYPES OF ANTENNAS OF THE SAME LENGTH
(L = 40 mm)

Type of Antenna	Feed Horn	Gain (dB)	BW_H (Degrees)	SL_H (dB)
Straight Rod	N	11.9	32.4	-2.5
Both-Tapered Rod	N	15.6	32.2	-10.0
Both-Tapered Rod	Y	17.7	28.5	-18.7
E-Plane Tapered Rod	Y	18.5	25.5	-13.1* -22.6
Zucker's Maximum Gain Rod	Y	19.1	15.9	-6.2

*This is the level of a shoulder in the main lobe.
See Figure 15 for detail.

III. PERIODICALLY MODULATED SURFACE WAVE ANTENNA

A. Basic Theory

Examples of periodically modulated surface-wave antennas and the coordinate system used in this chapter are shown in Figure 20. The angle measured from the x-y plane, denoted as θ', is sometimes used for theoretical work, while the angle θ from the endfire direction is used for radiation pattern measurements.

This type of antenna is no more than a linear array whose radiation elements are excited along the rod by a traveling wave, which is basically a surface wave [15], [16]. If we neglect the mutual coupling effect between elements, the backward waves reflected at discontinuities and additional perturbations at the feed end and the terminal end, the array factor, AF, is known to be

$$AF = A_o \sum_{k=o}^{N-1} Z^k = A_o \frac{1 - Z^N}{1 - Z} \tag{4}$$

where A_o is a constant, N is the number of elements and Z is a complex number given as

$$Z = \alpha e^{j\psi} \tag{5}$$

A real number α, where $0<\alpha<1$, is the amplitude ratio of two adjacent elements which characterizes the attenuation of the excitation along the rod, and ψ is a variable such that

$$\psi = k_o d \left(\cos 0 - \frac{\beta z}{k_o}\right) \tag{6}$$

where k_o and β_z are the phase constants in free space and in the dielectric rod in the z-direction, respectively, and d is the spacing of the perturbations. Then, the radiation intensity function of the array factor is obtained;

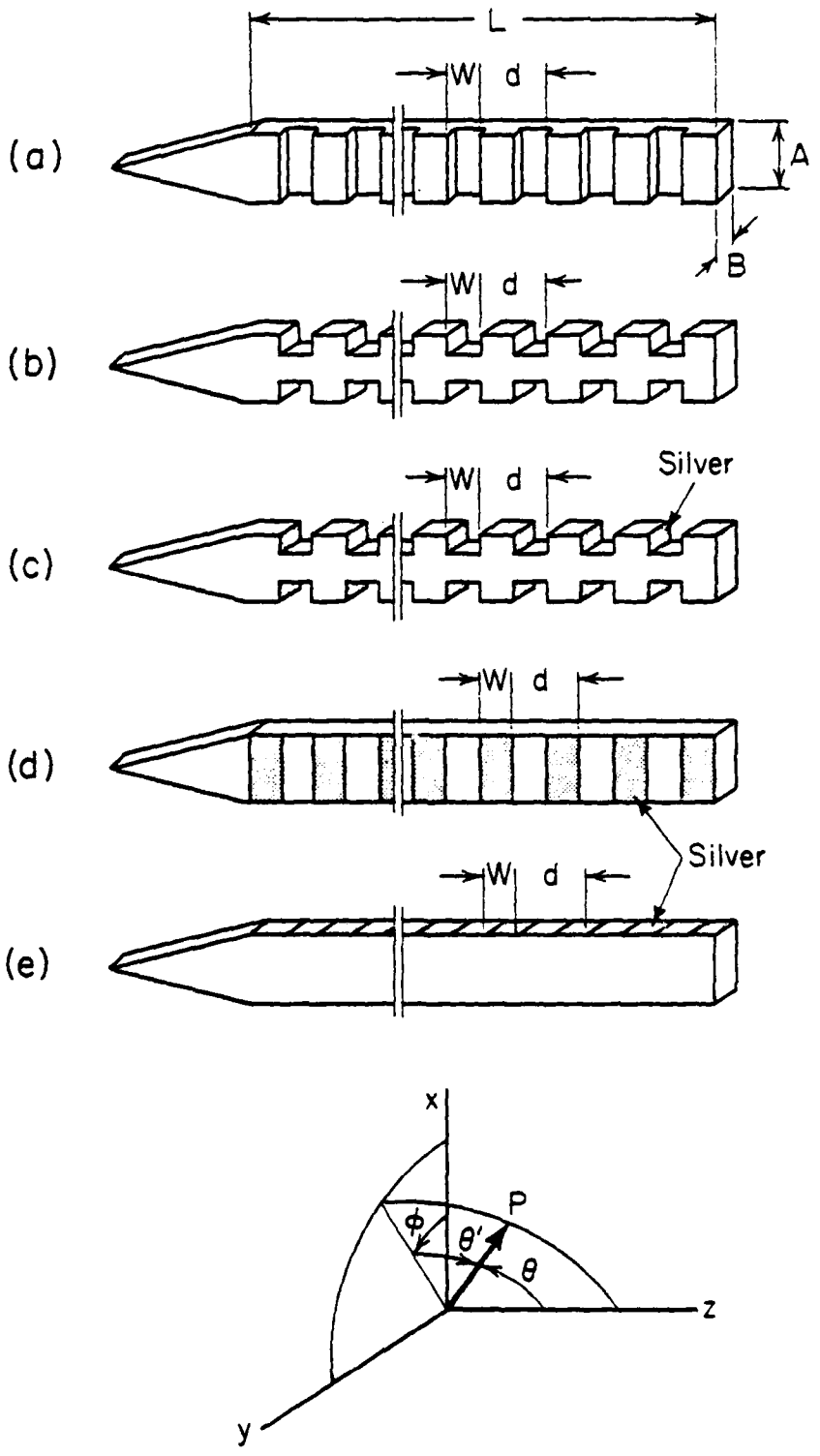

Figure 20. Examples of periodically modulated surface-wave antennas and the coordinate system.

$$|AF|^2 = |A_o|^2 \frac{(1-\alpha^N \cos N\psi)^2 + \alpha^{2N} \sin^2 N\psi}{(1-\alpha\cos\psi)^2 + \alpha^2 \sin^2\psi} \tag{7}$$

The largest beam occurs when $\psi = 2m\pi$ ($m = 0, \pm1, \pm2, \ldots$), where m is the space harmonic number. Therefore,

$$\cos\theta = \sin\theta' = \frac{\beta z}{k_o} + m\frac{2\pi}{k_o d} \tag{8}$$

$$\theta' = \sin^{-1}\left(r + m\frac{\lambda_o}{d}\right) \tag{9}$$

where $r \equiv \beta_z/k_o = \lambda_o/\lambda_z$ (10)

and $\left|r + m\frac{\lambda_o}{d}\right| \leq 1$ (11)

The formula (9) shows that the main beam is a conical beam. Since r is always larger than 1 for a dielectric rod, m has to be negative and it is most likely to be -1 for the rod whose relative dielectric constant is not too large.

From the viewpoint of grating lobes (see Appendix B), it is best to choose $m = -1$ and the period d from the regions (1) through (4), or preferably only (1), in Figure 21. Figure 21 tells us how to choose the material and the spacing of the perturbations. If r is larger than 5, which is equivalent to using a material whose relative dielectric constant is sufficiently larger than 25, the main beam can be directed to any angular direction without seeing any portion of a grating lobe by choosing d in the region (1). If r is between 3 and 5, we will see a part of, or at most a half of, a grating lobe near the backfire direction when d is chosen in region (2). This phenomenon reduces the practical range of the main beam direction. If r is between 2 and 3, the limitation occurs in either endfire or backfire direction. If r is smaller than 2, we will always see a partial grating lobe in the endfire and/or backfire direction

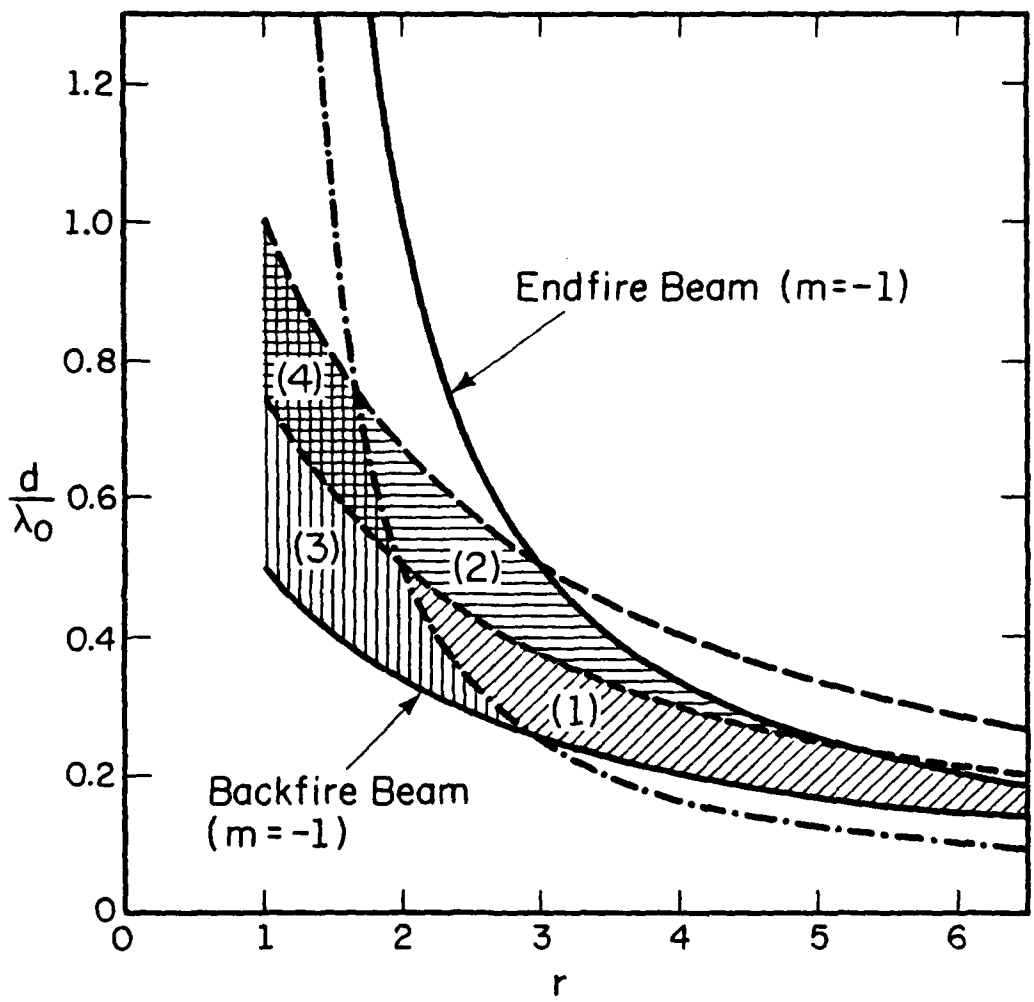

Figure 21. The range of d/λ_0.

(1) Main beam only
(2) (4) Main beam with a partial backward grating lobe
(3) (4) Main beam with a partial forward grating lobe

and the available angular range of the main beam is very limited.

In order to predict the pattern, especially the pattern in the main beam cone, of this type of antenna more precisely, we need to know the type and dimensions of each perturbation. To model the perturbation properly, the array factor derived before is multiplied by the space factor of each perturbation and by the element pattern of an infinitesimal dipole.

The estimation of phase constant βz and the attenuation constant α along the rod is not attempted in this work. They are obtained experimentally or calculated roughly by applying some conventional methods [7], [9], [10] to a hypothetical unperturbed rod which may or may not have the same cross-sections as the rod.

B. Design Factors

Design factors for a periodically modulated surface wave antenna are summarized in Table 3.

C. Experimental Procedure

Since the mechanism of perturbation is not clear, several types of antennas with different kinds of perturbation were fabricated on a cut-and-try basis and the radiation pattern of each antenna was recorded by using the same equipment that is described in Section C of this chapter. Radiation patterns are recorded not only in the E- and/or H-plane, but also in the main beam cone for the different polarizations, E_ϕ and E_θ, because each type of perturbation has its own space factor. Considering the asymmetry of some types of perturbation, each radiation pattern was recorded over 360 degrees.

Only polyethylene ($\varepsilon_r = 2.33$) was used as the material of all the rods for this primary study, which results in a radiation pattern having

TABLE 3

DESIGN FACTORS FOR A PERIODICALLY MODULATED SURFACE WAVE ANTENNA

Common Factors:

- Frequency or frequency range
- Metal waveguide (cross-sectional dimensions)
- Material of the rod (dielectric constant, loss tangent, etc.)

Transitions Factors:

- Length of transition
- Taper of the metal waveguide
- Taper of the rod

Feed Factors:

- Type of the feed
- Dimensions of the feed
- Taper of the rod

Main Antenna Factors:

- Cross-sectional dimensions of the rod
- Type of perturbation
- Position of perturbation
- Period of perturbation
- Number of perturbation (length of the rod)
- Dimensions of perturbation

at least a partial grating lobe in the forward direction (see Figure 21). Since many early experimental results showed unnecessary lobes in the endfire direction, which are much higher than the expected partial grating lobe, one of the objectives was set to lower those endfire lobes by a proper design. It was also attempted to grasp the general features of this type of antenna at millimeter wave frequencies.

D. Experimental Results

D.1 Antenna with notches

Early experiments were made using notches cut into the dielectric rod as perturbations, examples of which are shown in Figures 20(a) and (b). The antennas were fabricated so as to fit an RG 99/U waveguide and were inserted directly into the metal waveguide. An H-plane pattern of an antenna, such as shown in Figure 20(b), with 29 pairs of notches (d = 2.54 mm, W = 1.6 mm, depth of notches = 0.76 mm) is presented in Figure 22. The conical main beam at $\theta = 106$ degrees is very narrow in the r-θ plane, and very wide in the cone divided into four beams at $\phi=0$, $\pi/2$, and $3\pi/2$. But, the level of unnecessary lobes near the endfire direction is very high. Since the pattern of the latter resembles the pattern shown in Figure 9, it is concluded that these lobes are mostly due to the residual surface wave energy. A longer antenna with 105 pairs of notches yielded a main beam 8.5dB greater than the residual surface-wave lobes. Plating the inside walls of the notches with silver (Figure 20(c)) suppressed the residual lobes to 11.9 dB below the main beam level, but the suppression was not satisfactory.

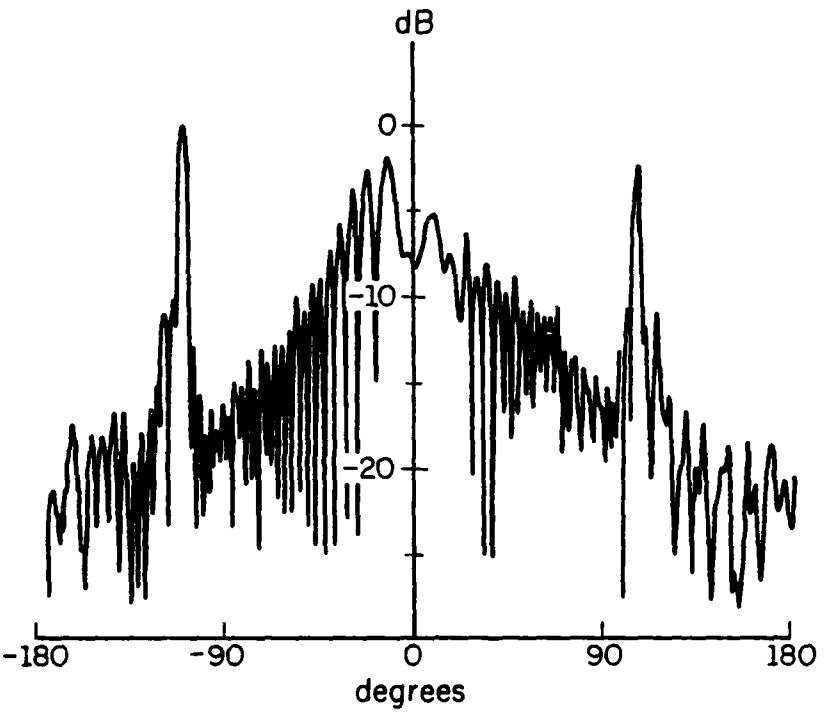

Figure 22. Radiation pattern of periodically modulated surface-wave antenna with notches.

D.2 Antenna with silver strips

After trying various kinds of perturbations, we found that we can get very efficient perturbations by placing silver strips periodically on one of the broader sides of the rods. It was also found experimentally that a width of strip equal to half of the period was the most effective radiator giving the best pattern. The radiation pattern of this type of antenna, (d) in Figure 20, with 29 strips (d=2.54 mm, w=1.27 mm) is shown in Figure 23. The main beam is 17.2 dB higher than the undesired lobes near the endfire direction; furthermore, the endfire radiation is no longer attributable to residual surface waves. Since the partial grating lobes are expected to be lower, we need to find another explanation for the lobes near the endfire direction.

It is also possible to place the strips on the narrower side of the rod as shown in Figure 20 (e). Since the space factor of each strip and the element pattern of an infinitesimal dipole are different in each case, they have different radiation patterns in the main beam cone as shown in Figure 24 and Figure 25. If the strips are on the narrower side, the polarization characteristic is complicated. It is also found that the beam from the side of the strips which is open to the air has a lower gain and a wider beam width than the beam from the other side of the strips. If narrower beams are needed not only in the r-o plane but also in the main beam cone, the cross-sectional dimensions may be changed, which requires a taper at the feed and some care to keep the rod single moded. If the rod is multimoded, we may see more unnecessary lobes.

Measurement of the near field of an antenna with 29 strips, 1.27 mm wide and spaced with a period of 2.54 mm on a broader side showed that the field decreased exponentially along the rod at 4.5 dB per centimeter. This

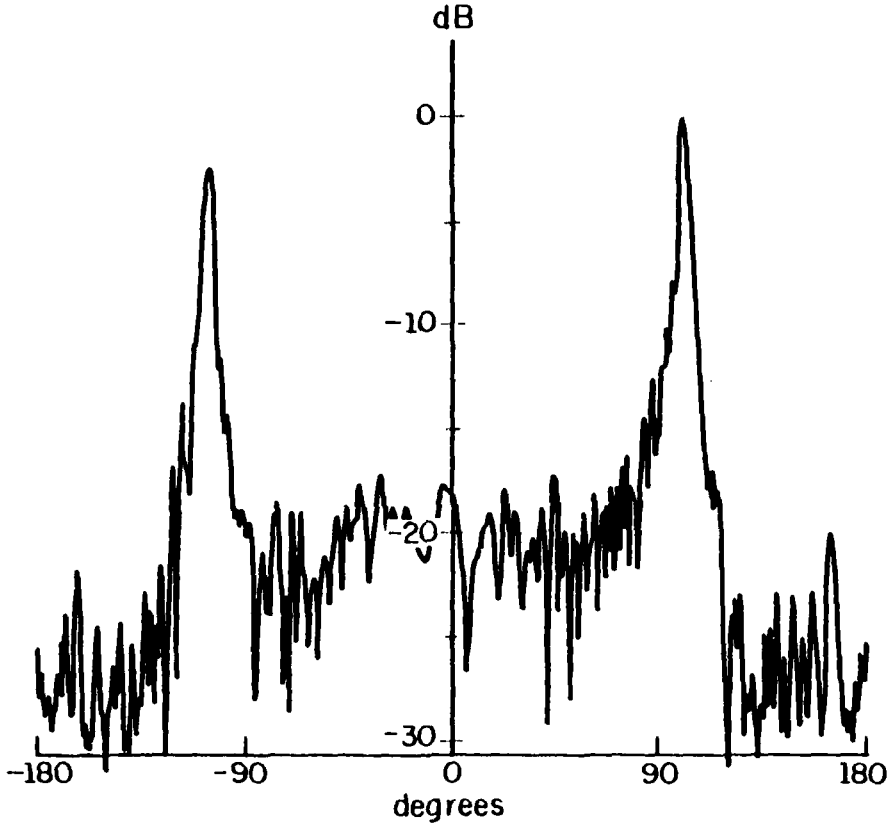

Figure 23. Radiation pattern of periodically modulated surface-wave antenna with silver strips.

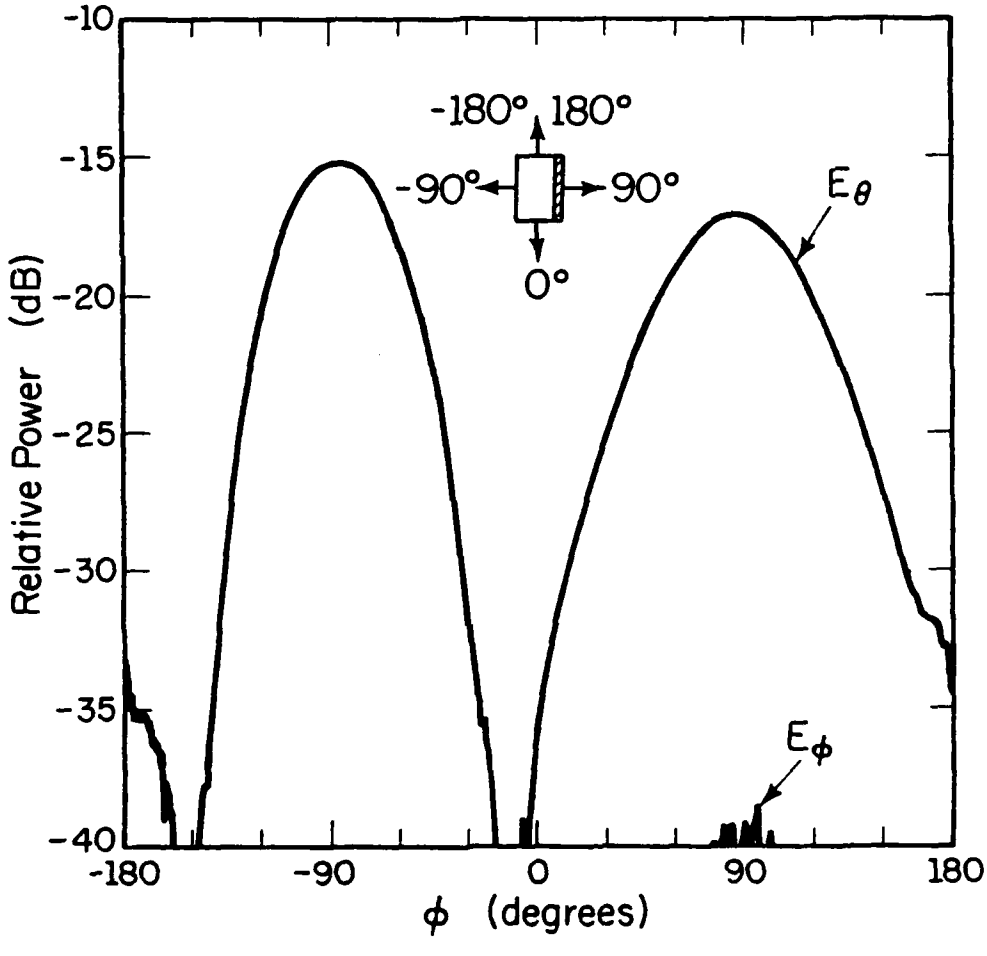

Figure 24. Radiation pattern for different polarizations in the main beam cone (θ = constant).

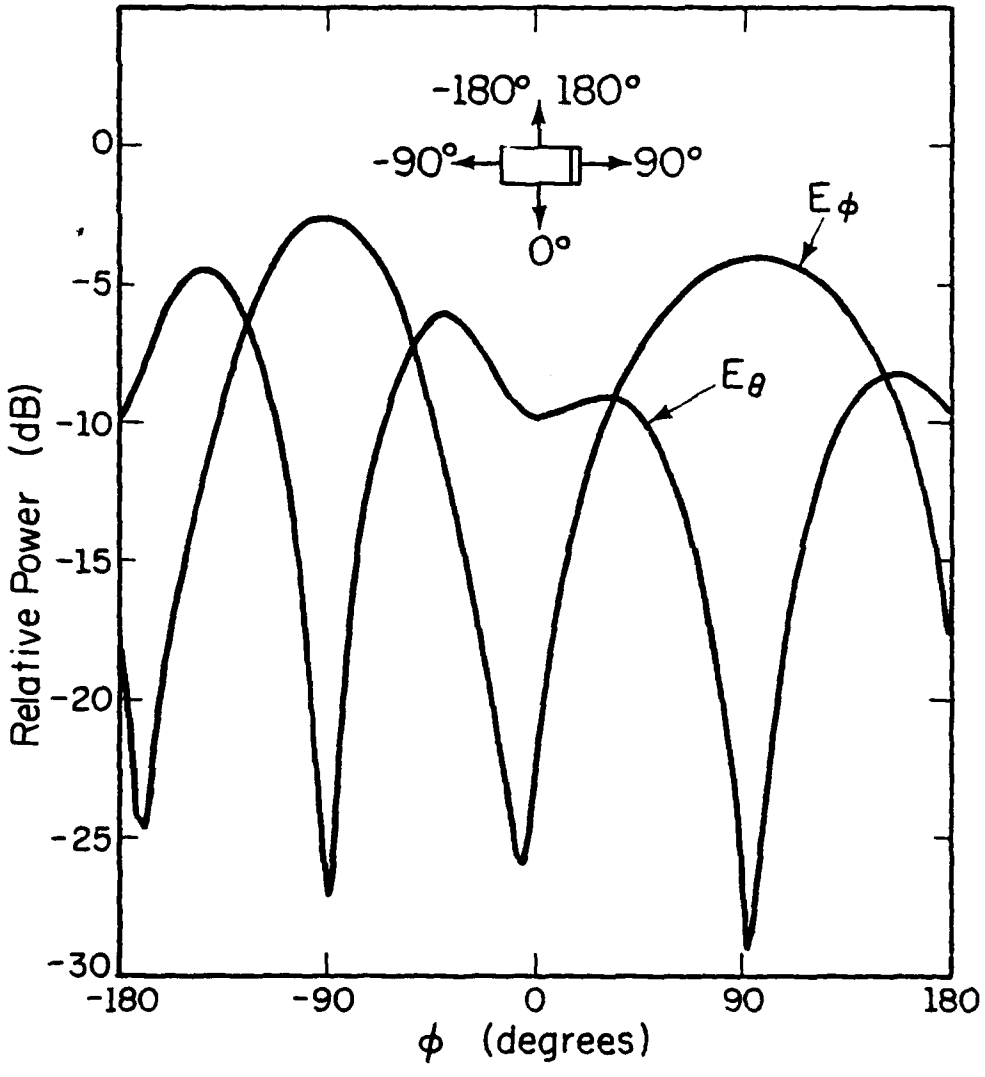

Figure 25. Radiation pattern for different polarizations in the main beam cone (θ = 110 degrees).

implies that only 0.06 percent of the energy is left inside the rod at the terminal end and the radiation from an abrupt discontinuity at this point is negligible.

D.3 Dependency on the number of perturbations

Even if the strips on a broader side of the rod, which are the most effective perturbation in this work, are used as perturbations, unnecessary lobes near the endfire direction are fairly high when the number of the strips is not enough. On the other hand, we might waste the strips near the terminal end, because they are weakly excited if there are too many strips.

Figure 26 shows the measured results of the relative level of unnecessary lobes at 80 GHz. It shows that a 1.27 mm wide strip is a more efficient radiator than a 0.76 mm wide strip and that the suppression of unnecessary lobes is not significant for 1.27 mm wide strips when the number of the strips is more than about 25. We can truncate the rod at this point with very little sacrifice on the radiation pattern. Since the curve shows a relatively sudden bend, the same measurement will be useful in the practical design of this type of antenna.

D.4 Beam steering

The Equation (9) indicates the possibility of beam steering by changing the frequency because both r and λ_o are frequency dependent. If the frequency increases, r increases and λ_o decreases. Since the space harmonic number m is always negative for the dielectric antennas, the angle θ' increases.

Although Figure 21 shows that higher dielectric constant material is necessary to get a wide range of conical beam angle, only polyethylene ($\varepsilon_r = 2.33$) was used for this primary study.

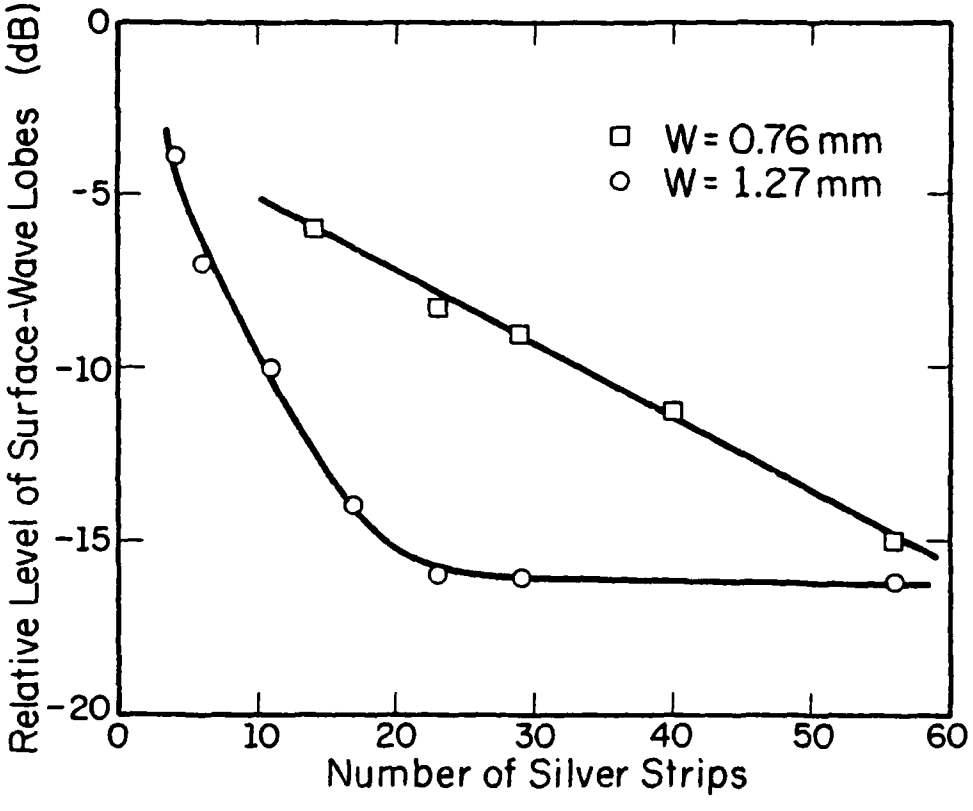

Figure 26. Suppression of unnecessary lobes.

Experimental results for the case in which the metal strips are printed on the broader side of the rod are shown in Figure 27 together with the semi-theoretical curves. The practical angular range in which there is only one space harmonic is between -70 to +10 degrees in this case. The angle changes more rapidly in the backward angle than near the broadside. Since the element pattern of the perturbation used here has nulls at $\theta' = \pm\pi/2$, the range is limited near the backfire direction. If the strips are placed on a narrower side, the same limitation will not occur.

The curves in Figure 27 are semitheoretical curves calculated by introducing a hypothetical unperturbed dielectric rod whose cross-section is A x B* instead of the real cross-section A x B. Although Itanami and Shindo's approximation method [10], which is simple enough to use a hand calculator but is not so accurate in a single-moded region, is used to calculate a parameter r, the agreement between experimental and calculated results is fairly good throughout the measured range. The equivalent height of the rod, B*, is the value which is calculated back by using the Equation (9) and at least one measured angle at the known frequency in the range. Once B* is obtained, r can be calculated throughout the range by using Itanami and Shindo's method again and the Equation (9) predicts the direction of the beam. Using the same technique, A*, A* with B* = A*/2 and ε_r* were tried and B* was found to be the best. B* depends on the type and dimensions of the perturbation and it varied from 1.45B to 1.52B for each curve shown in Figure 27.

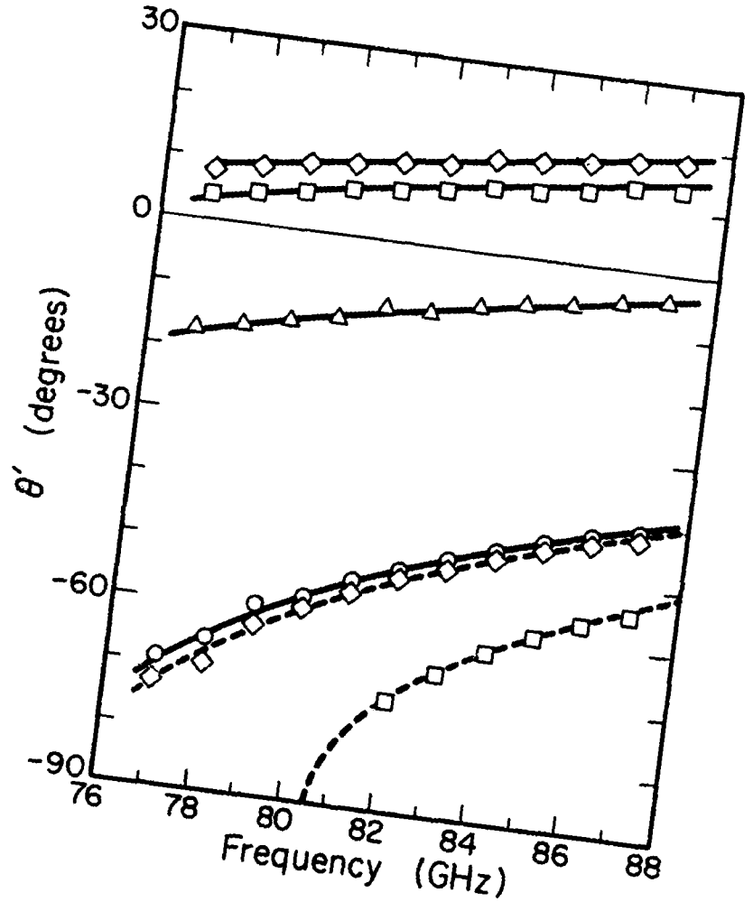

Figure 27. Beam steering:

Theoretical curves for A x B*

—— m = -1

---- m = -2 (grating lobe)

Experimental Results

d = 0.79 mm

d = 3.30 mm

d = 2.54 mm

d = 3.56 mm

IV. CONCLUSIONS

Experimental study on two classes of dielectric antennas with rectangular cross-section was conducted at millimeter-wave frequencies.

Two types of dielectric rod antennas are promising, one of which is a linearly tapered rod and the other is a so-called maximum gain antenna. The former has remarkably low side lobes and very steep off-main beam attenuation. The latter, if it is designed properly, has a gain which is almost proportional to the length, so that a fairly high gain can be achieved. Since this type of antenna becomes thinner and thinner as the gain increases, some mechanical support is required for high gain antennas. For both types of rod antennas, a feed horn is necessary to get good results, and tapering in only the E-plane improves the mechanical strength and sometimes the radiation characteristics, too. In general, a material with a dielectric constant as low as possible is preferable for this class of antennas.

A primary study on a periodically modulated surface-wave antenna was carried out as another class of antenna. The main beams are in a θ = constant cone, very narrow in the r-θ plane and fairly wide in the main beam cone. main beam can be steered by changing the frequency. The cross-section of the rod has to be chosen so that single-mode operation is maintained throughout the range, and the spacing of the perturbation has to satisfy some conditions in order not to have grating lobes and to have wide beam-steerability. The number of the perturbation is chosen so that the residual surface-wave radiation is sufficiently suppressed. Silver strips periodically placed on one side of the rod are very efficient radiators. In general, a material with a higher dielectric constant seems to be better in terms of wide-beam steerability, although a proper transition and feed have to be developed.

V. APPENDICES

A. Appendix A: Method of Design for Maximum-Gain Antennas

The method of design proposed here is based on the Zucker's design principle [5] applied to a rod shown in Figure A-1. Only E-plane taper is applied in the feed and main antenna sections.

Zucker's design principles determine L_f, L_r and B' when the relative dielectric constant E_r, the cross section of the metal waveguide A and B, and the required gain or beamwidth are given. Introducing the local wave number k_z along the rod, the phase difference conditions, which are the most important principles, can be interpreted as follows:

$$\int_o^{L_f} (k_z - k_o)\, dz = \frac{\pi}{3} \qquad (A.1)$$

and

$$\int_o^{L} (k_z - k_o)\, dz = \rho\pi \qquad (A.2)$$

where ρ depends on L and is between 1/3 and 1. The second formula is represented in Figure A-2 by a solid line. If both formulae are satisfied, the maximum gain and the minimum half-power beamwidth, which are shown in Figure A-3, are obtained.

Zucker also says that the length of the terminal taper L_e should be approximately 0.5λ and that it is desirable to have the horn just beyond the end of the feed taper, i.e., $L_h \sim 1.1\, L_f$.

In our problem, the Zucker's principles are applied as follows: Since we use only E-plane taper, we can use the approximation that k_z in the feed section changes linearly from $k_z(0)$ to $k_z(L_f)$ (see Figure 14); and, since the height of the rod B' in the main antenna section must be

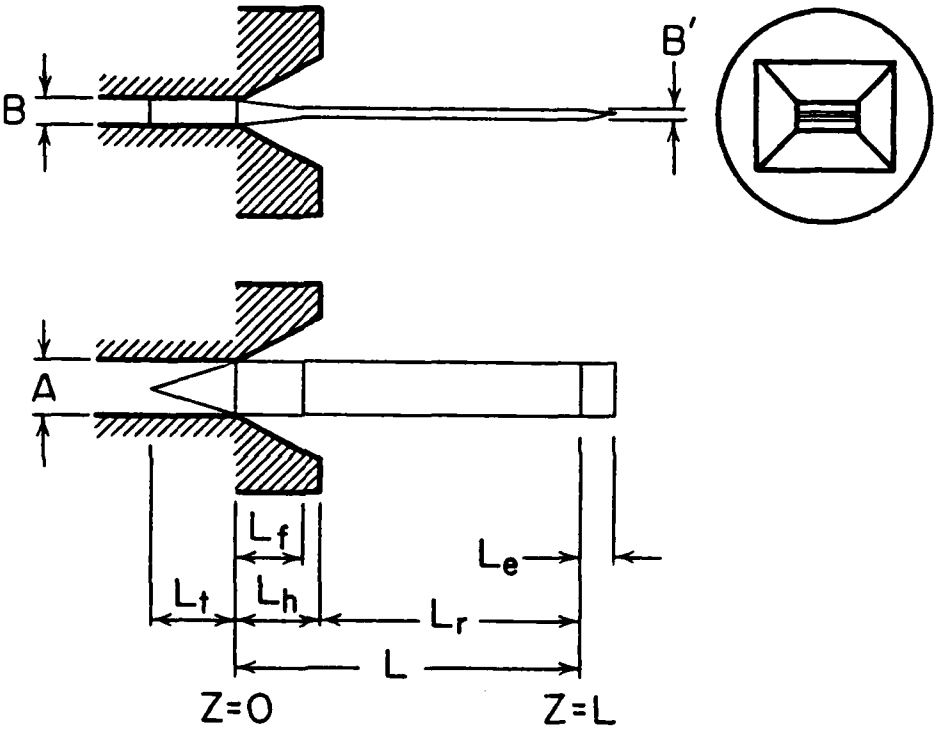

Figure A-1. Configuration of maximum gain antenna.

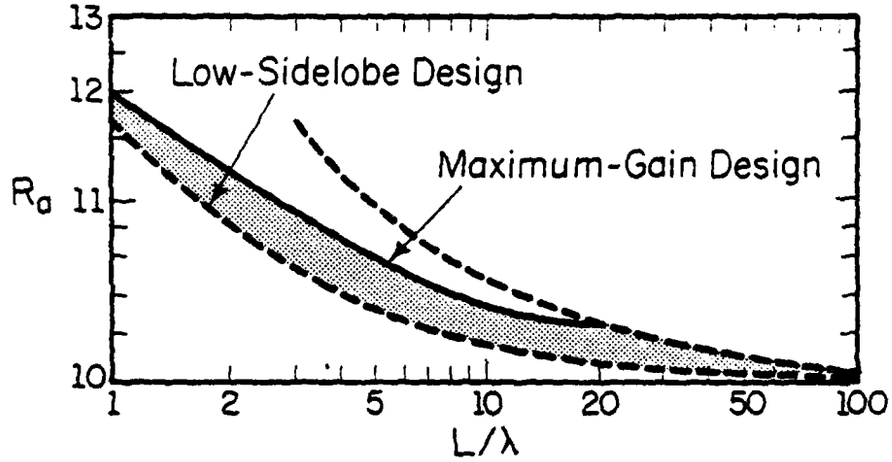

Figure A-2. Design curve 1.

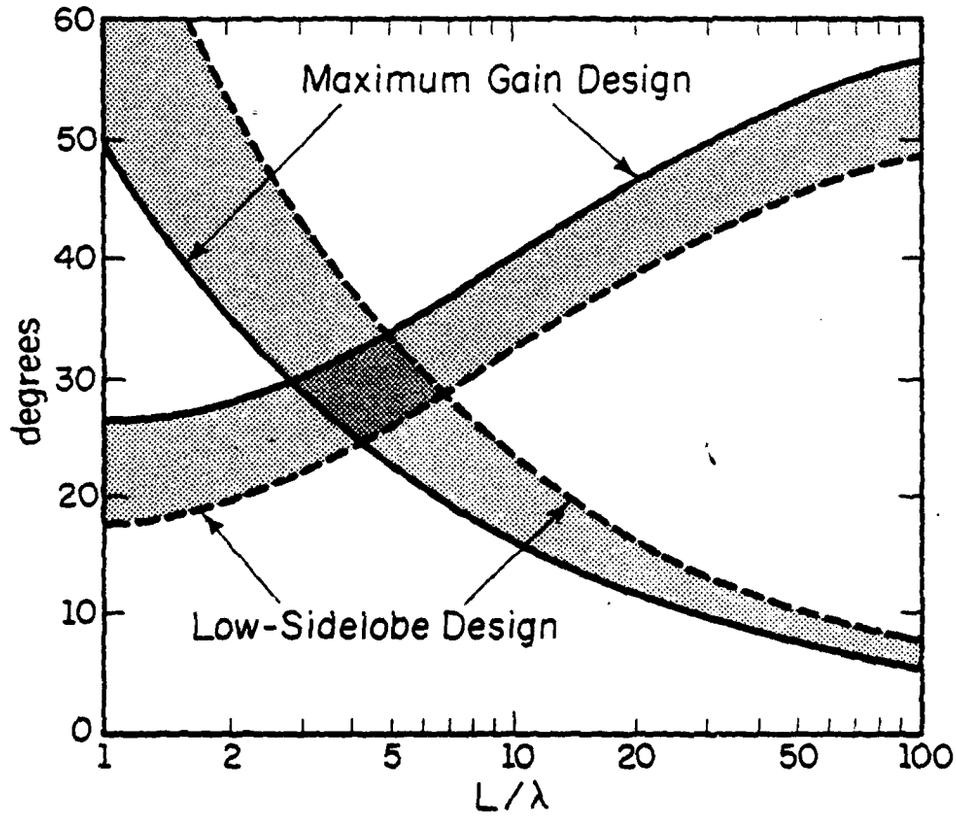

Figure A-3. Design curve 2.

very small, as long as the gain is not too low, we can neglect the terminal taper. We define:

$$R_o \equiv \frac{k_z(0)}{k_o} \tag{A.3}$$

$$R_r \equiv \frac{k_z(L_f)}{k_o} \tag{A.4}$$

$$R_a \equiv \frac{\overline{k}_z}{k_o} = \frac{1}{L}\int_o^L \left(\frac{k_z}{k_o}\right) dZ \tag{A.5}$$

where R_a is obtained from Figure A-2.

Applying the Zucker's principles, we obtain

$$\frac{2\pi}{\lambda_o}\left(\frac{R_o + R_r}{2} - 1\right)L_F = \frac{\pi}{3} \tag{A.6}$$

and $$\left(\frac{R_o + R_r}{2}\right)L_F + R_r\,(L - L_F) = r_a L \tag{A.7}$$

Solving these and choosing L_F in (0,L),

$$L_F = \frac{1}{2}\,(C_1 - \sqrt{C_1^2 - 4C_2}) \tag{A.8}$$

where $$C_1 = \frac{\lambda_o + 6(R_o + R_a - 2)L}{6(R_o - 1)} \tag{A.9}$$

$$C_2 = \frac{\lambda_o L}{3(R_o - 1)} \tag{A.10}$$

and $$R_r = \frac{\lambda_o}{3L_F} - R_o + 2 \tag{A.11}$$

Then, we can determine B′ so that $k_z(Z) = R_r k_o$ for $L_f \leq z \leq L$.

For example, in our standard case,

$f = 81.5$ GHz

$\lambda_o = 3.68$ mm

E_r = 2.33

A = 3.10 mm

B = 1.55 mm

Then, R_o = 1.203 by using the method of effective dielectric constant (see Figure 14). If we choose L = 40 mm (L/λ_0 = 10.87), Figure A-2 gives us R_a = 1.034. Using the formula derived before,

L_f = 5.46 mm

R_r = 1.022

Using Figure 14 again, we determine B′:

B′ = 0.65 mm

Figure A-3 shows that this antenna would have the gain of 20.2 dB and the beamwidth of 16 degrees.

B. Appendix B: Proper Range of Spacing of Perturbations

At the main beam of a periodically modulated surface wave antenna,

$$\psi = \frac{2\pi}{\lambda_o} d\ (\cos 0 - r) = 2m\pi,\ (m = 0, \pm 1, \pm 2\ldots) \tag{A.12}$$

therefore, $$\cos 0 = \sin 0' = r + m \frac{\lambda_o}{d} \tag{A.13}$$

and $$\left| r + m \frac{\lambda_o}{d} \right| \leq 1 \tag{A.14}$$

Since r is larger than 1, m has to be negative and we define a positive integer n:

$$n = -m \tag{A.15}$$

Equation (A.14) can be rewritten as:

$$\frac{n}{r+1} \leq \frac{d}{\lambda_o} \leq \frac{n}{r-1} \qquad \text{(Condition 1)} \tag{A.16}$$

In order to have only one space harmonic in the visible region, d/λ_o has to be larger than the upper limit of the $(n-1)^{\underline{th}}$ space harmonic and smaller than the lower limit of the $(n+1)^{\underline{th}}$ space harmonic.

So, $$\frac{n-1}{r-1} < \frac{d}{\lambda_o} < \frac{n+1}{r+1} \qquad \text{(Condition 2)} \tag{A.17}$$

Under the above condition, we may still see a part of, or at most a half of, the adjacent grating lobes.

In order not to see any portion of the grating lobes, the edges of the visible range in ψ have to be between $-(2n-1)\pi$ and $-(2n+1)\pi$ and we obtain

$$\frac{2n-1}{2(r-1)} < \frac{d}{\lambda_o} < \frac{2n+1}{2(r+1)} \qquad \text{(Condition 3)} \tag{A.18}$$

The range of d/λ_o for n = 1 is shown in Figure 21, which shows that we can choose any main beam direction if r is larger than the value at which the upper limits of (A.16) and (A.18) coincide. This value is calculated to be (4n + 1) and it is minimum when n = 1. Since high dielectric constant material causes much difficulty in most cases, it is desirable in realizing this type of antenna to choose n = 1, i.e., m = -1.

VI. LIST OF REFERENCES

[1] ANDERSON, J.B., "Radiation from surface-wave antennas," Electron. Lett., Vol. 3, No. 3, June 1967, pp. 251-252.

[2] KIELY, D.G., "Dielectric aerials" (Methuen Monograph, 1953).

[3] HORTON, C.W., KARAL, F.C., Jr., and McKINNEY, C.M., "On the radiation patterns of dielectric rods of circular cross section — The $TM_{0,1}$ mode," App. Phys., Vol. 21, December 1950, pp. 1279-1283.

[4] HORTON, C.W., and McKINNEY, C.M., Jr., "An experimental investigation of the dielectric rod antenna of circular cross section excited in the dominant mode," J. App. Phys., Vol. 22, No. 10, October 1951, pp. 1246-1249.

[5] ZUCKER, F.J., "Surface and leaky-wave antennas," in JASIK (Ed.): Antenna Engineering Handbook (McGraw-Hill, 1961), ch. 16.

[6] GOELL, J.E., "A circular-harmonic computer analysis of rectangular dielectric waveguides," The Bell Syst. Tech. J., September 1969, pp. 2133-2160.

[7] KNOX, R.M. and TOULIOS, P.P., "Integrated circuits for the millimeter through optical frequency range," Proc. Symp. Submillimeter Waves, New York, NY, March 1970.

[8] YANG, P., "A new method for the analysis of dielectric waveguides for millimeter wave and optical integrated circuits," Technical Report, Coordinated Science Laboratory, University of Illinois, Urbana, IL, May 1978.

[9] MARCATILI, E.A.J., "Dielectric rectangular waveguides and directional coupler for integrated optics," The Bell Sys. Tech. J., September 1969, pp. 2071-2102.

[10] ITANAMI, T. and SHINDOS, S., "Channel dropping filter for millimeter-wave integrated circuits," IEEE Trans. Microwave Theory Tech., Vol. MTT-26, No. 10, October 1978, pp. 759-764.

[11] FELSEN, L.B., "Electromagnetics properties of wedge and cone surface with a linearly varying surface impedance," IRE Trans. Antennas Propagat., Vol. AP-7, December 1959, pp. S231-S243.

[12] FELSEN, L.B., "Radiation from a tapered surface wave antenna," IRE Trans. Antennas and Propagat., Vol. AP-8, November 1960, pp. 577-586.

[13] WEEKS, W.L., "Antenna engineering," New York: McGraw-Hill, 1968, pp. 244-249.

[14] TRINH, T.N., MALHERBE, J.A.G., and MITTRA, R., "A metal-to-dielectric waveguide transition with application to millimeter-wave integrated circuits," to appear.

[15] ITOH, T., "Application of gratings in a dielectric waveguide for leaky-wave antennas and band-reject filters," IEEE Trans. Microwave Theory Tech., Vol. MTT-25, No. 12, December 1977, pp. 1134-1138.

[16] KLOHN, K.L., HORN, R.E. and JACOBS, H. and FREIBERGS, E., "Silicon waveguide frequency scanning linear array antenna," IEEE Trans. Microwave Theory Tech., Vol. MTT-26, No. 10, October 1978, pp. 764-773.